Photomodulation of Transport Rates in Liquid Membranes Containing Photoactive Carriers

Teresa L. Longin and Carl A. Koval*

Department of Chemistry and Biochemistry, University of Colorado, Boulder, Colorado 80309-0215

Richard D. Noble*

Department of Chemical Engineering, University of Colorado, Boulder, Colorado 80309-0424

Received: September 3, 1997

A steady-state model describing photofacilitated transport in liquid membranes is used to consider photoactive carriers with a wide range of thermodynamic and kinetic properties in order to calculate photoinduced modulation in the transport rates of solutes, a phenomenon known as photomodulation. Most experimental and theoretical studies have focused on systems in which strongly binding forms of the carrier and carrier−solute complex absorb light to convert to weakly binding forms. For such systems, absorption of light can cause photomodulation increases up to a factor of 3. However, the maximum photoefficiencies are only a few percent, where photoefficiency is defined as the difference between the flux under illumination and in the dark divided by the incident photon flux. Conversely, if the weakly binding forms of the carrier and complex are photoactive, photomodulation increases of a factor of 20 can be achieved, along with photoefficiencies well over 10%. This study provides guidelines for the selection of carriers for future experimental investigations of photofacilitated liquid membranes.

Introduction

Facilitated transport in liquid membranes is a rich field of study.[1,2] The advantages of facilitated transport can be extended if the binding properties of the carrier can be modulated with light.[3] In the most commonly studied type of photofacilitated membrane (depicted in Figure 1a), a strongly binding form of a carrier absorbs light (generally of a fairly narrow bandwidth) and converts to a form that has a low binding affinity for a solute. Shining light of the appropriate wavelength on the sweep interface of the membrane effectively enhances the release rate of solute and thus creates a steep concentration gradient of solute at that interface. This, in turn, increases the total flux of solute across the membrane, a phenomenon referred to as photofacilitation.

Photofacilitation in liquid membranes provides temporal and spatial control over the transport properties of the membranes. The flux of solute across the membrane can be adjusted from being limited by physical solubility to much higher values by the choice of an appropriate light intensity. This enhanced flux can be made to occur at specific locations on the membrane surface using a focused source. If the carrier is chemically selective for a particular solute in the feed, the selectivity will be enhanced along with the total flux of solute through the liquid membrane. Thus, the magnitude and position of the solute flux as well as the selectivity of the membrane can be controlled by light. Selective delivery of solutes such as drugs or monomers becomes possible with photofacilitation. In addition, a photoactive membrane could also be used as a photochemical sensor.

The desirable properties for photofacilitated membranes are somewhat different than those for simple thermal facilitated membranes. In thermal facilitated membranes, the focus is on obtaining the highest possible solute fluxes. While this would also be a major concern in photofacilitated membranes, the ability to modulate the flux also becomes important. Thus, the change in transport properties between the membrane in the dark and under illumination, or the degree of photomodulation, is also of interest. In addition, the photoefficiency of the membrane in terms of flux of solute as a function of photon flux is also an important concern.

A number of studies have investigated the possibilities of photofacilitated liquid membranes.[4−14] Most of these studies demonstrated photofacilitation with varying degrees of success, and most focused on membranes in which the strong forms of the carrier and complex were photoactive. However, the selection of highly optimal systems for photofacilitation has been hampered by an incomplete understanding of the various parameters important in photofacilitated transport and their relationships to each other.

Jain and Schultz conducted a mathematical analysis of photofacilitated transport using a simplified model in which only one form of the carrier and complex existed.[15] They assumed that the decomplexation rate was enhanced by a light intensity dependent rate and that the light intensity was constant across the illuminated portion of the membrane rather than decaying exponentially in intensity across the membrane. The study reported herein incorporates a more general model for photofacilitation and a more thorough treatment of the interaction of light with the carrier and carrier−solute complex. Both thermodynamic and kinetic parameters are investigated, and the optimal conditions necessary for photofacilitation and photomodulation are examined.

In a previous study,[16] photomodulation effects were explored for theoretical membrane systems in which the strong forms of the carrier and complex were photoactive and optimized for thermal transport. In this study, the focus was on exploring parameters which gave high degrees of photomodulation and high photoefficiencies. In addition, membranes in which the weak forms of the carrier and complex were photoactive were

S1089-5647(97)02878-2 CCC: $15.00
Published on Web 01/15/1998

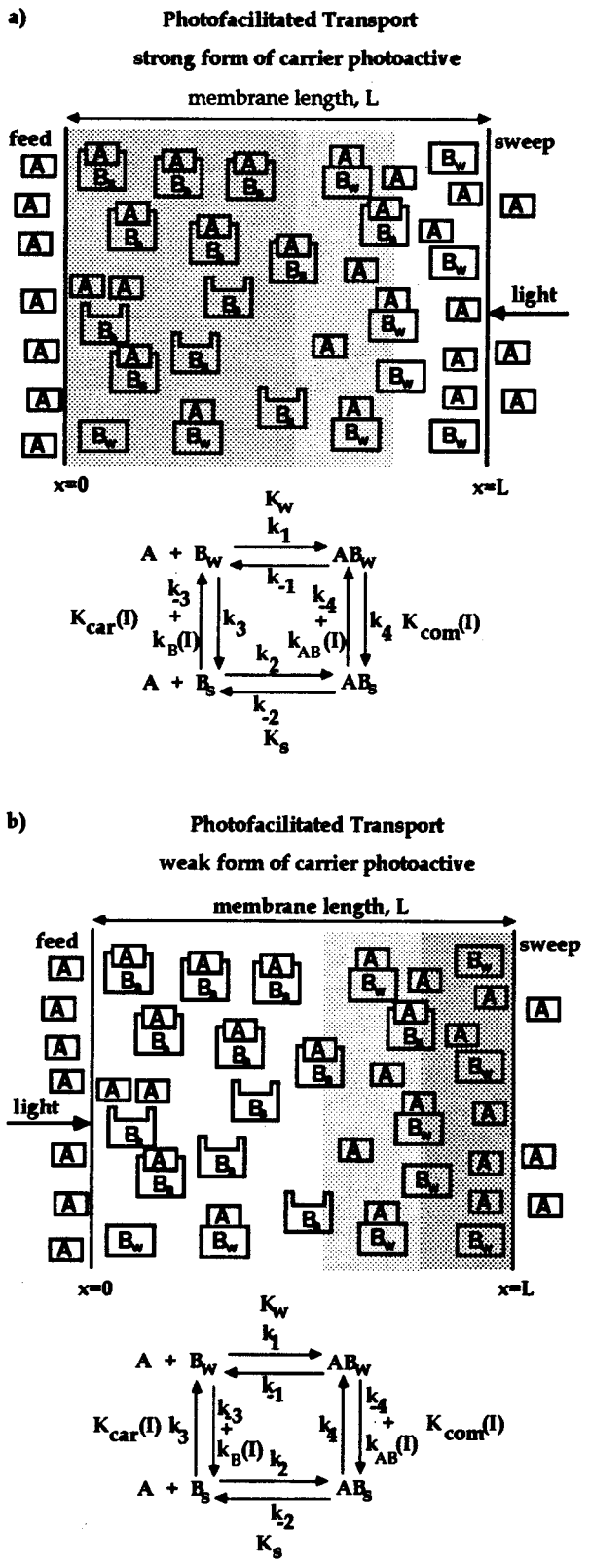

Figure 1. Schematic depictions of photofacilitated liquid membranes and the reaction schemes used as the models for photofacilitated transport in liquid membranes. The shading represents different levels of light intensity, where no shading indicates highest light intensity and the dark shading indicates lowest light intensity. (a) A photofacilitated liquid membrane in which light initiates conversion of the strongly binding forms of the carrier and carrier−solute complex to the weakly binding forms. (b) A photofacilitated liquid membrane in which light initiates conversion of the weakly binding forms of the carrier and complex to the strongly binding forms.

investigated, along with the more conventional membranes in which the strong forms of the carrier and complex were photoactive.

Model

Figure 1 depicts the reaction schemes used as the models for photofacilitated transport in this study. The carrier can exist in the form of four species. The uncomplexed carrier can be in a weakly binding form, B_w, or a strongly binding form, B_s. The carrier−solute complex is either a weakly bound form, AB_w, or a strongly bound form, AB_s.

$$A + B_w \underset{k_{-1}}{\overset{k_1}{\rightleftharpoons}} AB_w \qquad K_w = \frac{k_1}{k_{-1}} \tag{1}$$

$$A + B_s \underset{k_{-2}}{\overset{k_2}{\rightleftharpoons}} AB_s \qquad K_s = \frac{k_2}{k_{-2}} \tag{2}$$

In the model depicted in Figure 1a, where the strong forms of the carrier and complex are photoactive, the conversion of weak forms to strong forms is assumed to be a purely thermal process, while the conversions of strong forms to weak forms have both thermal rate constants (k_{-3} and k_{-4}) and light intensity dependent rate constants ($k_B(I)$ and $k_{AB}(I)$).

$$B_w \underset{k_{-3}+k_B(I)}{\overset{k_3}{\rightleftharpoons}} B_s \qquad K_{car}(I) = \frac{k_3}{k_{-3}+k_B(I)} \tag{3}$$

$$AB_w \underset{k_{-4}+k_{AB}(I)}{\overset{k_4}{\rightleftharpoons}} AB_s \qquad K_{com}(I) = \frac{k_4}{k_{-4}+k_{AB}(I)} \tag{4}$$

The subscripts "car" and "com" denote parameters for the carriers and complexes, respectively. The parameters K_s, K_w, $K_{car}(I)$, and $K_{com}(I)$ can be considered to be equilibrium constants under dark conditions. Under steady-state illumination, the interconversion constants become position-dependent.

For the model depicted in Figure 1b, the weak forms of the carrier and the carrier−solute complex are photoactive. In this case, the conversion rates of strong forms to weak forms are considered to be purely thermal, while the conversion rates of weak forms to strong forms have both a thermal and a light intensity dependent component.

$$B_s \underset{k_{-3}+k_B(I)}{\overset{k_3}{\rightleftharpoons}} B_w \qquad K_{car}(I) = \frac{k_3}{k_{-3}+k_B(I)} \tag{5}$$

$$AB_s \underset{k_{-4}+k_{AB}(I)}{\overset{k_4}{\rightleftharpoons}} AB_w \qquad K_{com}(I) = \frac{k_4}{k_{-4}+k_{AB}(I)} \tag{6}$$

Note that the definitions of the "equilibrium" constants for interconversion are still the rate constants for conversion of photoinactive forms to photoactive forms divided by the rate constants (both thermal and light intensity dependent) for conversion of the photoactive forms to the photoinactive forms.

In this model, the rate constants and the equilibrium constants for the binding of carrier to solute are not directly affected by light. Light does affect the relative concentrations of the strong forms and the weak forms of the carrier and complex. This enables the separate examinations of thermodynamic and kinetic characteristics.

The light intensity dependent rate constants are defined as simple linear functions of quantum yield for conversion, molar absorptivity coefficient, and incident light intensity.

$$k_B(I) = \Phi_B E_B I_0 \tag{7}$$

$$k_{AB}(I) = \Phi_{AB} E_{AB} I_0 \tag{8}$$

The important light-dependent parameters, denoted as η_{car} and η_{com}, are the ratios of the light-dependent rate constants to the thermal rate constants for interconversion between the strong and weak forms of the carrier and complex.

$$\eta_{car} = \frac{\Phi_B E_B I_0}{k_{-3}}, \quad \eta_{com} = \frac{\Phi_{AB} E_{AB} I_0}{k_{-4}} \tag{9}$$

Here, Φ represents the quantum yield for conversion of the photoactive form of carrier (or complex) to the photoinactive form of carrier (or complex) in units of mol of photoactive form converted/mol of photons absorbed. E represents molar absorptivity in units of cm^2/mol. I_0 is the incident light intensity. For ease of solution and characterization, many of the variables are grouped together into dimensionless parameters. A detailed description and list of the various parameters are given in the Appendix to this paper.

The concentrations of each species in the membrane are controlled by reaction kinetics (as depicted in Figure 1a,b) and by steady-state diffusion. The equations that describe the concentration profiles of each species at steady state are determined from Fick's second law.[16] The profile for the light intensity is calculated from Beer's law in its differential form.[16] The equations and parameters are converted to dimensionless form to clarify and generalize photofacilitation effects. The dimensionless forms of the mass transport equations, the light intensity profiles, and the boundary conditions are all described in a previous paper.[16] Some details are also described in the Appendix to this paper. The equations do not contain any expressions for a thermal gradient; thus the results apply only to membranes maintained at a constant temperature. It should also be noted that ionic effects were neglected, since solute ions partition into the membrane in the form of ion pairs. Ion pairs maintain electroneutrality; thus the Nernst−Planck term is zero and Fick's laws of diffusion are sufficient to describe the system.[17,18]

The concentration of the solute within the membrane is normalized by the solute concentration at the feed interface, $[A]_0$.

$$\bar{A} = \frac{[A]}{[A]_0} \tag{10}$$

For all simulations carried out in this study, the concentration of solute at the sweep interface was set to zero. The concentrations of each form of the carrier (including each form of the complex) are normalized to the total carrier concentration, C_T. For example:

$$\overline{B_w} = \frac{[B_w]}{C_T}, \quad \overline{AB_w} = \frac{[AB_w]}{C_T} \tag{11}$$

The decomplexation rate constants are related to diffusion coefficients by

$$\epsilon_w = \frac{D_{AB}}{L^2 k_{-1}}, \quad \epsilon_s = \frac{D_{AB}}{L^2 k_{-2}} \tag{12}$$

where D_{AB} is the diffusion coefficient of the complex and L is the membrane thickness. These parameters relate reaction times to diffusion times. Small ϵ's indicate large rate constants and rapid reaction rates. The binding equilibrium constants are made dimensionless by adjusting for the concentration of solute at the feed interface.

$$K_w^d = \frac{k_1}{k_{-1}}[A]_0, \quad K_s^d = \frac{k_2}{k_{-2}}[A]_0 \tag{13}$$

Finally, there is parameter α that relates the mobility of the carrier (in all forms) to the mobility of the solute in the membrane.

$$\alpha = \frac{D_{AB} C_T}{D_A [A]_0} \tag{14}$$

For high facilitation, the mobility of the carrier should be much greater (by at least an order of magnitude) than the mobility of the solute.[19] That is generally experimentally achieved by having a very high concentration of the carrier in the membrane relative to the concentration of the solute in the membrane.

There are dimensionless kinetic parameters that relate reaction time for interconversion to diffusion time. In the dark, those parameters have the forms

$$\epsilon_{car_0} = \frac{D_{AB}}{L^2 k_{-3}}, \quad \epsilon_{com_0} = \frac{D_{AB}}{L^2 k_{-4}} \tag{15}$$

Under illumination, the thermal rate constants for interconversion are enhanced by the light intensity dependent rates, and the parameters become

$$\epsilon_{car}(I) = \frac{D_{AB}}{L^2(k_{-3}+k_B(I))} = \frac{\epsilon_{car_0}}{1+\eta_{car}\bar{I}},$$

$$\epsilon_{com}(I) = \frac{\epsilon_{com_0}}{1+\eta_{com}\bar{I}} \tag{16}$$

where $\bar{I}$ is the normalized light intensity. The equilibrium constants that describe the relative concentrations of each form of the carrier and complex in the dark have the forms

$$K_{car_0} = \frac{k_3}{k_{-3}}, \quad K_{com_0} = \frac{k_4}{k_{-4}} \tag{17}$$

Under illumination, the equilibrium constants become light intensity dependent:

$$K_{car}(I) = \frac{k_3}{k_{-3}+k_B(I)} = \frac{K_{car_0}}{1+\eta_{car}\bar{I}},$$

$$K_{com}(I) = \frac{K_{com_0}}{1+\eta_{com}\bar{I}} \tag{18}$$

Finally, there is a dimensionless parameter that involves the extent to which light is absorbed by each photoactive form of the carrier:

$$\beta_{car} = \tilde{E}_B C_T L, \quad \beta_{com} = \tilde{E}_{AB} C_T L \tag{19}$$

Here, $\tilde{E}$ represents molar absorptivity in units of L/(mol cm). Note that if a molecule has a low molar absorptivity coefficient, increasing the total carrier concentration or the membrane

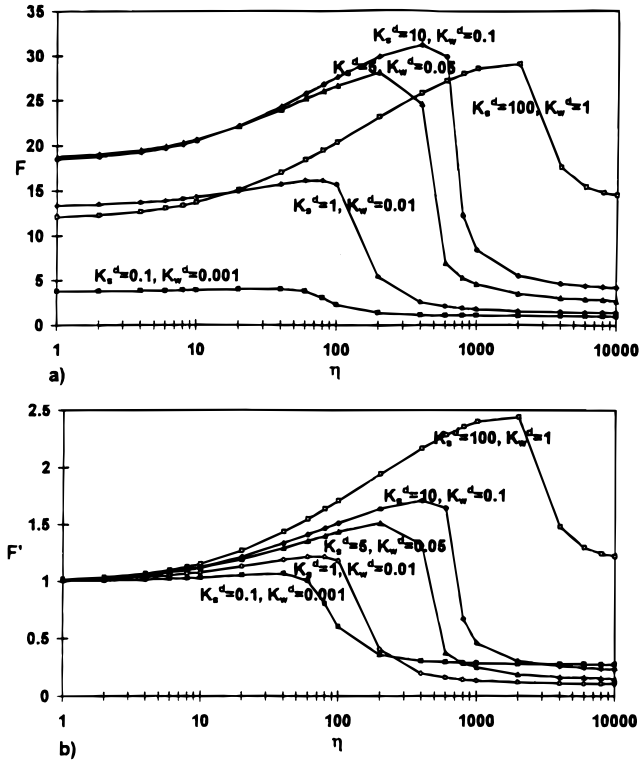

Figure 2. Plots of facilitation and photomodulation versus light intensity for different binding constants in liquid membranes in which the strong forms of the carrier and complex were photoactive. For all cases, $\alpha = 50$, $\beta = 10$, $\epsilon_s = \epsilon_w = 0.01$, $\epsilon_{car_0} = \epsilon_{com_0} = 0.01$, $K_{car_0} = 10$, and $K_{com_0} = 1000$. (a) Plots of facilitation factor, F, versus light intensity parameter, η, for various sets of binding constants. F is defined by eq 20 in the text. (b) Plots of the degree of photomodulation, F', versus η for various sets of binding constants. F' is defined by eq 21 in the text.

thickness has the same effect on the value of β as increasing the molar absorptivity coefficient.

Results and Discussion

Strong Forms of the Carrier and Complex Photoactive. Light Incident on Sweep Interface. For all the simulations carried out with strong forms of the carrier and complex photoactive, the light was incident on the sweep interface. The values of ϵ_s and ϵ_w were 0.01, values which correspond to fast decomplexation kinetics. Increasing the values of the decomplexation kinetic parameters always resulted in poor transport properties, even under illumination. The values of ϵ_{car_0} and ϵ_{com_0} were also 0.01, unless otherwise noted. The value of α was 50, which corresponds to high carrier mobility. The value of β was 10, unless otherwise noted; this value corresponds to a high molar absorptivity coefficient.

A. Effects of Complexation Constants. Figure 2 depicts the results of simulations for various combinations of K_s^d and K_w^d as K_s^d was shifted from the thermally optimal value of 5. For all combinations, the ratio of K_s^d/K_w^d was 0.01 and $K_{car_0} = 10$, resulting in a constant $K_{com_0} = 1000$. For each figure, each point represents the results of a simulation for a given set of parameters at a particular value of the light intensity parameter, η. The lines simply connect the points and are intended as a guide to the eye.

The reactions of interest were those shown in eqs 1 and 2:

$$A + B_w \underset{k_{-1}}{\overset{k_1}{\rightleftharpoons}} AB_w$$

and

$$A + B_s \underset{k_{-2}}{\overset{k_2}{\rightleftharpoons}} AB_s$$

The principle parameters being varied were the complexation (forward) rate constants, while the decomplexation (reverse) rate constants and interconversion kinetics were left unchanged.

A convenient term for characterizing facilitation is the facilitation factor, F, defined as the ratio of the total dimensionless flux of A with carrier present to the total dimensionless flux of A without carrier present at the same concentration driving force across the membrane.

$$F = \frac{N_{\bar{A},\text{carrier}}}{N_{\bar{A},\text{no carrier}}} \tag{20}$$

It is also convenient to define a facilitation factor that expresses the degree of photomodulation. This photomodulation facilitation factor can be defined as

$$F' = \frac{N_{\bar{A},\text{light}}}{N_{\bar{A},\text{dark}}} \tag{21}$$

That is, F' is the ratio of the total flux of solute obtained at a given light intensity parameter to the total flux of solute obtained in the dark ($\eta = 0$).

Figure 2a shows a plot of the facilitation factor, F, versus the light intensity parameter, η, for a range of K_s^d values of 100 to 0.1. Below a $K_s^d = 5$, facilitation factors were low and the degree of photomodulation was negligible. For $K_s^d = 5$ or greater, the facilitation factors were reasonably large and there was significant photomodulation.

The differences in degrees of photomodulation are shown in Figure 2b, which depicts F' versus η. Since F' is defined as the ratio of total flux of solute in the light to total flux of solute in the dark, it is an expression of degree of photomodulation. Note that for $K_s^d = 5$ and 10 (both of which are in the range for optimal thermal transport) the degree of photomodulation was about 1.5. However, for a $K_s^d = 100$, F' was almost 2.5. Thus, binding equilibrium constants greater than thermally optimal values provided greater degrees of photomodulation than will binding constants at or below values optimal for thermal transport.

The explanation for the higher degree of photomodulation for the large value of K_s^d is shown in Figure 3. For this large complexation constant, relatively little free solute existed in the membrane. In the dark ($\eta = 0$), this limited the concentration gradients of free solute at the sweep interface, providing a relatively low flux of solute across the membrane and a low facilitation factor.

The situation changed significantly as the light intensity was increased and the strong form of the complex was converted to the weak form at the sweep interface. The complexation rate for the weak form of the carrier was significantly lower than that of the strong form (as reflected by the difference in their binding constants), so the amount of free solute at the sweep interface built up, increasing the flux (see Figure 3a). As can be seen in the concentration profile for solute at the optimal light intensity, $\eta = 2000$, the amount of free solute in the membrane was much greater than in the dark, resulting in a much steeper concentration gradient at each interface, with a correspondingly greater total flux of solute. At much higher light intensities ($\eta = 10{,}000$), most of the strong forms of the carrier and complex were converted to the weak forms and the

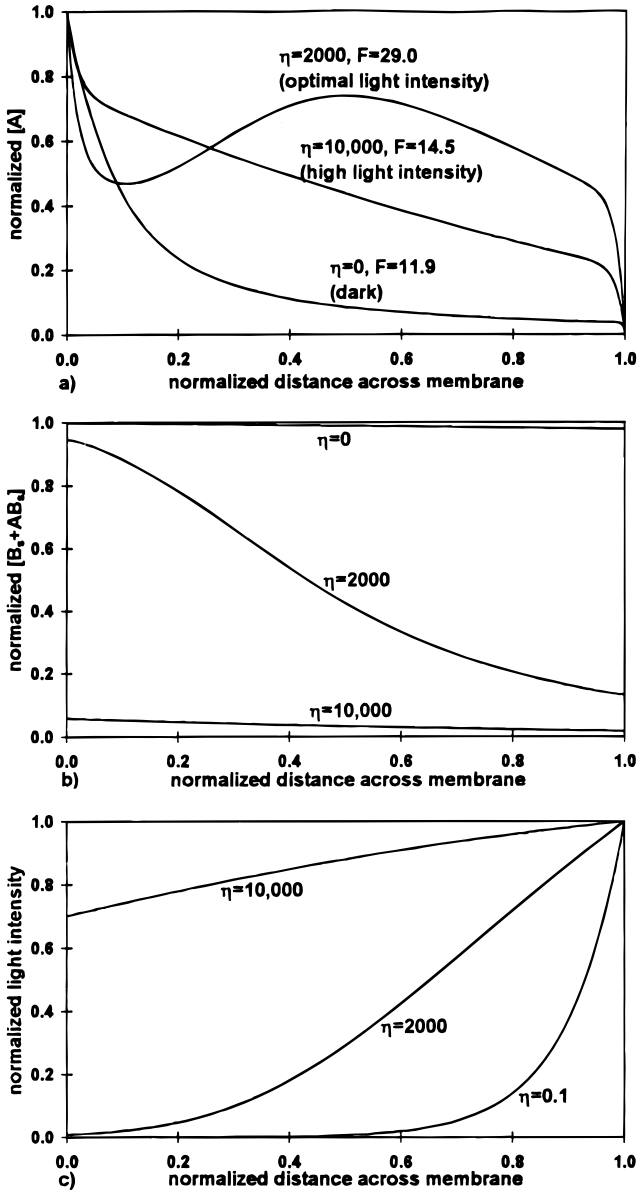

Figure 3. Normalized concentration and light intensity profiles across a membrane in which the strong forms of the carrier and complex were photoactive. For this membrane, $\alpha = 50$, $\beta = 10$, $\epsilon_s = \epsilon_w = 0.01$, $\epsilon_{car_0} = \epsilon_{com_0} = 0.01$, $K_{car_0} = 10$, $K_{com_0} = 1000$, $K_s^d = 100$, and $K_w^d = 1$. (a) Normalized concentration profiles for the solute, A, across the membrane at various light intensities. (b) Normalized concentration profiles for the sum of the strong forms of the carrier and complex ($B_s + AB_s$) across the membrane at various light intensities. (c) Normalized light intensity profiles across the membrane at various light intensities.

facilitation factor approached that for the weak form of the carrier (see Figure 3b).

It is interesting to note the shape of the light intensity profile at the optimal light intensity for photomodulation ($\eta = 2000$) versus the shape for lower light intensities (Figure 3c). At low light intensities, the light penetrated about halfway through the membrane before decaying to zero, as was expected for the chosen β ($\beta = 10$). However, at $\eta = 2000$, the light penetrated all the way across the membrane before decaying to zero. This particular pattern was previously observed in simulations of membranes in which the strong form of the carrier was optimized for thermal transport.[16] Indeed, for all simulations run for membranes in which the strong form of the carrier was photoactive, the light penetrated through the membrane and the intensity decayed to zero at the feed interface at the optimal light intensity for photomodulation. Past that optimal light intensity, light began to reach the feed interface, significantly depleting the strong forms of the carrier and complex at that interface and reducing the total flux of the solute.

One feature of all curves depicting degree of photomodulation as a function of light intensity (for example, see Figure 2b) was the rapid decrease in F' past the optimal light intensity. One way of achieving a significant degree of photomodulation (meaning a large change in the transport properties of the membrane) would be to modulate the light intensity between the optimal intensity and a slightly higher intensity. Larger changes in the transport properties of the membrane generally could be achieved in this way rather than by modulating between no light and the optimal light intensity. However, operating in the light intensity region at and above the optimal intensity means the photoefficiency would be very low.

B. Effects of Weak Complexation Constant. Truly optimal systems for photofacilitation would be photoefficient, providing large solute fluxes at low light intensity. A transport photoefficiency can be defined as

$$\Psi = \left(\frac{(\text{total flux A})_{\text{light}} - (\text{total flux A})_{\text{dark}}}{I_0} \right) \times 100 \qquad (22)$$

In the dimensionless parameters used in this study, the photoefficiency becomes

$$\Psi = \frac{\beta_{\text{com}} \epsilon_{\text{com}_0}}{\alpha \eta_{\text{com}}} (N_{\bar{A},\text{light}} - N_{\bar{A},\text{dark}}) \times 100 \qquad (23)$$

Under this definition, photoefficiencies can be negative, indicating reduced transport in the light.

Figure 4 shows the effect of varying K_w^d on the degree of photomodulation and photoefficiency for $K_s^d = 100$. In this case, the focus of the simulations was the reaction described by eq 1:

$$A + B_w \underset{k_{-1}}{\overset{k_1}{\rightleftharpoons}} AB_w$$

where the magnitude of k_1 was varied. As K_w^d increased, the maximum facilitation factor, degree of photomodulation, and photoefficiency decreased. This trend was not unexpected, in that an increase in K_w^d with no increase in ϵ_w corresponds to an increase in the complexation rate constant for the weak form of the carrier. That means that the weak form complexed a significant amount of the free solute, reducing the concentration of free solute at the sweep interface. This resulted in a decrease in the flux of solute across the sweep interface and a decrease in the total flux of solute across the membrane. Clearly, in order to achieve significant degrees of photomodulation and good photoefficiencies, the binding constant of the weak form of the carrier should be as low as possible.

C. Effects of Interconversion Equilibrium Constants. Changing the equilibrium constant between the strong and weak forms of the carrier would be expected to have a significant effect on the maximum facilitation factor obtained, the degree of photomodulation, and the photoefficiency. The reactions directly affected are the interconversion equilibria described in eqs 3 and 4:

$$B_w \underset{k_{-3}+k_B(I)}{\overset{k_3}{\rightleftharpoons}} B_s$$

and

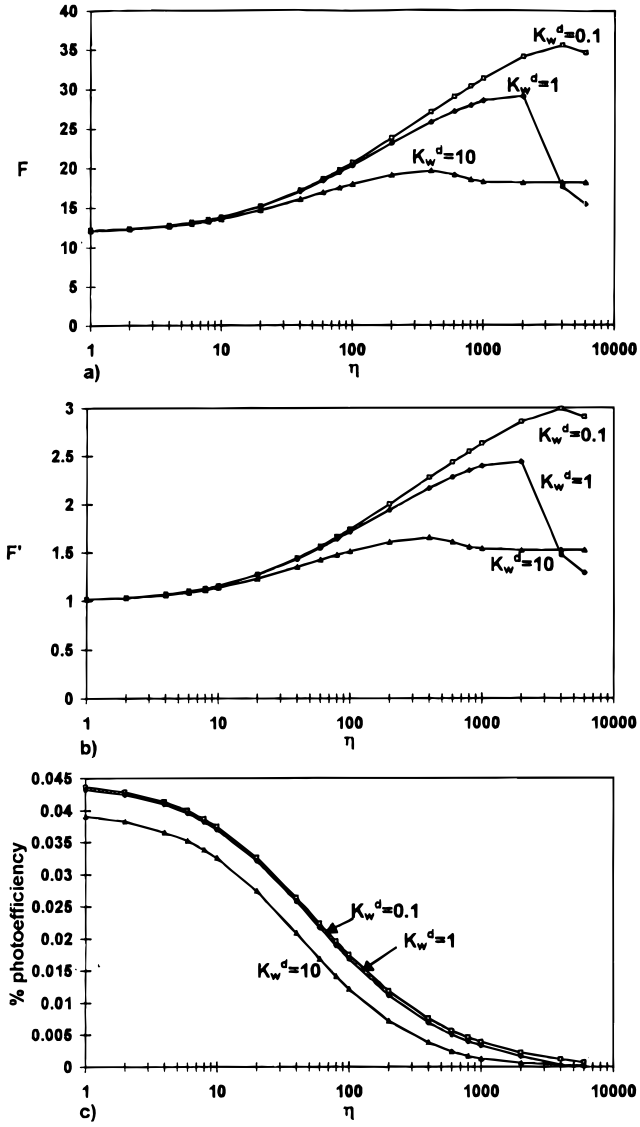

Figure 4. Plots of facilitation, photomodulation, and photoefficiency versus light intensity for various weak binding constants. For all cases, $\alpha = 50$, $\beta = 10$, $\epsilon_s = \epsilon_w = 0.01$, $\epsilon_{car_0} = \epsilon_{com_0} = 0.01$, $K_{car_0} = 10$, and $K_s^d = 100$. (a) Plots of facilitation factor, F, versus light intensity parameter, η, for various K_w^d. (b) Plots of degree of photomodulation, F', versus η for various K_w^d. (c) Plots of % photoefficiency versus η for various K_w^d. Photoefficiency is defined by eq 22 in the text.

$$AB_w \underset{k_{-4}+k_{AB}(I)}{\overset{k_4}{\rightleftharpoons}} AB_s$$

Lowering K_{car_0} results in a direct decrease in K_{com_0}, and the concentrations of the strong form of the carrier and complex will be lower relative to the concentrations of the weak forms. Figure 5 shows the results for simulations exploring this trend for $K_s^d = 100$ and $K_w^d = 0.1$, the combination of binding constants that showed the largest facilitation factor, degree of photomodulation, and photoefficiency.

As expected, decreasing K_{car_0} resulted in a decrease in both the maximum facilitation factor achieved and the degree of photomodulation. Since the concentrations of the strong forms of the carrier and complex decreased with decreasing K_{car_0}, the amount of bound solute released upon photoconversion of the strong form of the complex to the weak form also decreased. This resulted in lower concentration gradients of free solute at the interfaces and lower fluxes of solute.

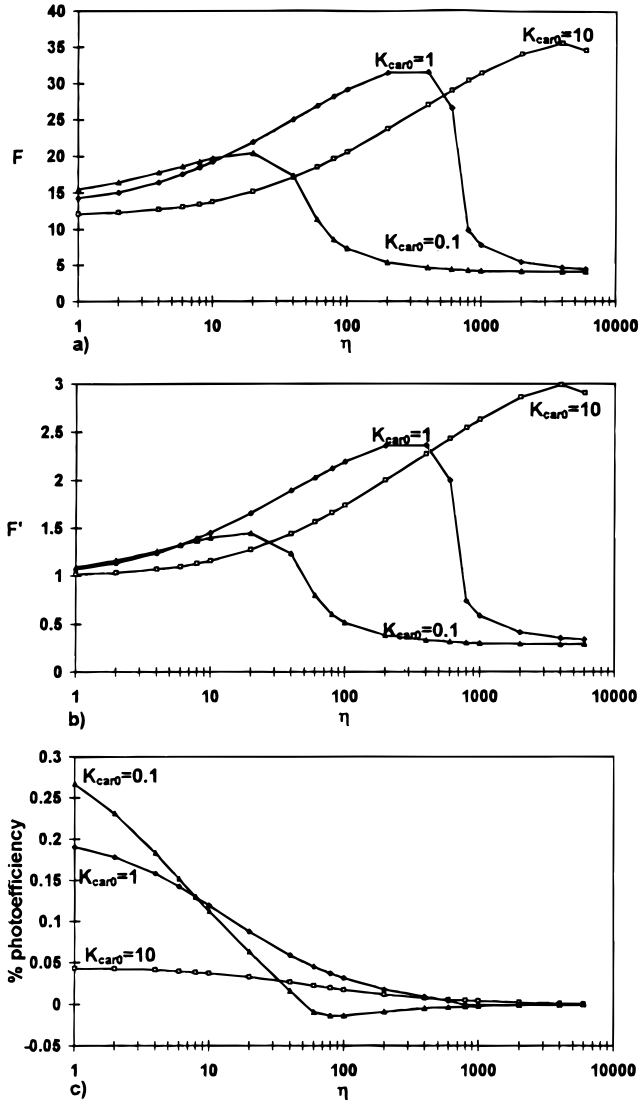

Figure 5. Plots of facilitation, degree of photomodulation, and photoefficiency versus light intensity for various interconversion constants, K_{car_0}. For all cases, $\alpha = 50$, $\beta = 10$, $\epsilon_s = \epsilon_w = 0.01$, $\epsilon_{car_0} = \epsilon_{com_0} = 0.01$, $K_w^d = 0.1$, and $K_s^d = 100$. (a) Plots of facilitation factor, F, versus light intensity parameter, η, for various K_{car_0}. (b) Plots of degree of photomodulation, F', versus η for various K_{car_0}. (c) Plots of % photoefficiency versus η for various K_{car_0}.

As can be seen in Figure 5a,b, reducing K_{car_0} also reduced the light intensity necessary to achieve the highest facilitation factor and degree of photomodulation. At low light intensities ($\eta < 10$), this resulted in a general increase in photoefficiency with decrease in K_{car_0}. At light intensity factors greater than 10, however, the photoefficiencies for $K_{car_0} = 0.1$ dropped below those for both $K_{car_0} = 1$ and $K_{car_0} = 10$. Conversely, the photoefficiencies for $K_{car_0} = 1$ stayed well above those for $K_{car_0} = 10$ until light intensity factors of over 100 were reached. Thus it seems that a $K_{car_0} = 1$ (meaning equal concentrations of strong and weak forms of the carrier in the dark) will provide membranes that have both a reasonably high degree of photomodulation and reasonably high photoefficiencies.

D. Effects of Interconversion Kinetics. Decreasing the rates of interconversion of the forms of the carrier and complex would be expected to increase photoefficiencies. Slow interconversion rates mean that each molecule of carrier or complex converted stays in the weak form longer, meaning that each photon absorbed is more effective. However, it was not intuitively clear what effect slowing the interconversion rates

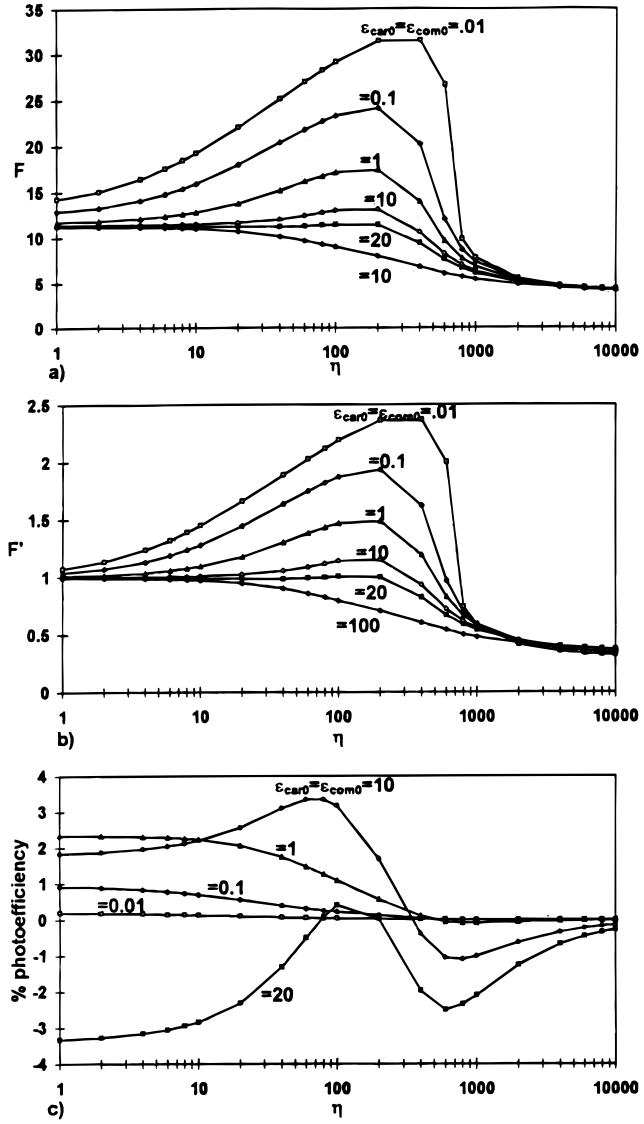

Figure 6. Plots of facilitation, degree of photomodulation, and photoefficiency versus light intensity as the thermal rates of interconversion between strong and weak forms were slowed. For all cases, $\alpha = 50$, $\beta = 10$, $\epsilon_s = \epsilon_w = 0.01$, $K_w^d = 0.1$, $K_s^d = 100$, $K_{car_0} = 1$, and $K_{com_0} = 1000$. (a) Plots of facilitation factor, F, versus light intensity parameter, η, for various interconversion rates. (b) Plots of degree of photomodulation, F', versus η for various interconversion rates. (c) Plots of % photoefficiency versus η for various interconversion rates.

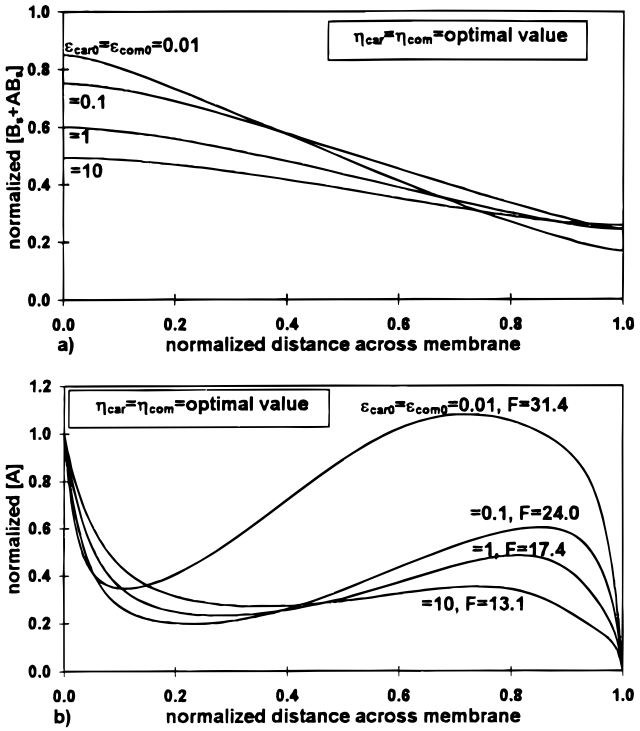

Figure 7. Normalized concentration profiles for various interconversion rates. For all cases, $\alpha = 50$, $\beta = 10$, $\epsilon_s = \epsilon_w = 0.01$, $K_w^d = 0.1$, $K_s^d = 100$, $K_{car_0} = 1$, and $K_{com_0} = 1000$. (a) Normalized concentration profiles for the sum of the strong forms of the carrier and complex ($B_s + AB_s$) for various interconversion rates at the optimal light intensity for photofacilitation at each rate. (b) Normalized concentration profiles for the solute, A, for various interconversion rates at the optimal light intensity for photofacilitation at each rate.

would have on transport of solute in general. Consequently, simulations were run in which the values of ϵ_{car_0} and ϵ_{com_0} were increased (meaning a decrease in the interconversion rates) with $K_s^d = 100$, $K_w^d = 0.1$, and $K_{car_0} = 1$.

The values of the facilitation factors and degrees of photomodulation are shown in Figure 6a,b. Generally, the facilitation decreased with increasing ϵ_{car_0} and ϵ_{com_0}. While this particular trend was not expected, it is easily explained by the concentration profiles for the total amount of strong form of the carrier at each value of ϵ_{car_0} and ϵ_{com_0}, as shown in Figure 7a. At the optimal light intensity for photofacilitation, the total concentration of the strong forms of the carrier decreased at the feed interface with increasing ϵ_{car_0} and ϵ_{com_0}. This resulted in a decrease in the amount of solute drawn into the membrane and then ultimately released at the sweep interface, as shown in Figure 7b. This resulted in decreasing solute concentration gradients with slower interconversion kinetics. Note that the light intensity values required for optimal photofacilitation were essentially the same for all values of ϵ_{car_0} and ϵ_{com_0}. Since the concentrations of the strong forms of the carrier and complex in the dark were about the same regardless of ϵ_{car_0} and ϵ_{com_0}, it took about the same amount of light intensity to produce the optimal amount of photoconversion for each value of ϵ_{car_0} and ϵ_{com_0}.

The increase in ϵ_{car_0} and ϵ_{com_0} did result in an increase in the photoefficiency, up to $\epsilon_{car_0} = \epsilon_{com_0} = 10$. Above that value, the interconversion rates slowed to the point that photobleaching began at very low light intensities, and the total flux of solute decreased from the dark value. This resulted in negative photoefficiencies at almost all light intensities.

E. Effects of Carrier Mobility. A few other parameters were also varied. Simulations were run in which the value of α was reduced from 50. Reducing α has the effect of reducing the total concentration of the carrier in the membrane relative to the concentration of free solute at the feed interface. Generally, reducing α reduces the facilitation factor, since there is less carrier in the membrane. Decreasing α would be expected to increase the photoefficiency, since decreasing the total amount of carrier means less light would be required to cause significant changes in the relative concentrations of the strong and weak forms.

As it turned out, the effects counteracted each other. Lowering α did decrease the light intensity required to achieve the maximum degree of photomodulation. However, it also resulted in a decrease in the extent of photomodulation. The end result was that the photoefficiency remained essentially constant as α was decreased. Since lowering α resulted in a decrease in both the maximum facilitation factor obtained and the degree of photomodulation without causing an increase in the photo-

TABLE 1: Strong Forms Photoactive, Light Incident on Sweep Interface

range of K_s^d	F_{max}	F'_{max}	% photoefficiency
<1	<10	~1	<0.1
1−5	10−25	~1−1.5	<0.1
5−10	25−35	1.5−2	<0.1
>10	>25	>2	<0.1

TABLE 2: Strong Forms Photoactive, Light Incident on Sweep Interface

parameter varied	F_{max}	F'_{max}	% photoefficiency	section
decrease K_w^d	increase	increase	increase	B
decrease K_{car_0}	decrease	decrease	increase (at low light intensities)	C
increase ϵ_{car_0} and ϵ_{com_0}	decrease	decrease	increase, then decrease	D
decrease α	decrease	decrease	no change	E
increase β_{car} and β_{com}	increase	increase	increase	F

efficiency, it is optimal to have a high α, that is, a high total concentration of carrier relative to solute.

F. Effects of Molar Absorptivity Coefficients. From the definition of photoefficiency (eq 23), increasing β (the normalized absorptivity coefficient) should increase the photoefficiency. Increasing the molar absorptivity coefficient means more of the light is absorbed closer to the illuminated interface. In a previous study, the effect of β was examined in detail for liquid membranes in which the strong form of the carrier was photoactive and optimized for thermal transport.[16] It was found that a minimum value of 10 for β was necessary to achieve significant photofacilitation. Increasing β increased the maximum facilitation factor, the degree of photofacilitation, and the photoefficiency. Similar dependencies on β were found for the various sets of parameters studied. However, at the higher binding constants, increasing β resulted in an increase in the optimal light intensity parameter.

G. Summary. The following tables summarize the results of the simulations run in this study. Tables 1 and 2 apply to photofacilitated liquid membranes in which the strong forms of the carrier and complex are photoactive and light is incident on the sweep interface. Table 1 summarizes general results for small K_w^d (<1) and fast interconversion kinetics. Table 2 lists qualitative trends in the maximum facilitation factor, the maximum degree of photomodulation, and the photoefficiency obtained as the listed parameters were varied.

These results suggest some of the properties that should be sought in photoactive carriers. Primarily, the binding constant for the strong forms of the carrier should be as large as possible ($K_s^d > 10$), and the binding constant for the weak forms of the carrier should be as small as possible ($K_s^d < 1$). A value of K_{car_0} close to 1 will provide a good balance between the maximum facilitation factor, maximum degree of photomodulation, and the photoefficiency. The interconversion kinetic factors, ϵ_{car_0} and ϵ_{com_0}, should be about 0.1, meaning the interconversion time is about 10 times faster than the diffusion time. However, even membranes with highly optimal parameters will only exhibit degrees of photomodulation of less than five with low photoefficiencies.

Weak Forms of the Carrier and Complex Photoactive. Light Incident on Feed Interface. Very little research has been carried out on liquid membranes in which the weakly binding forms of the carrier and complex are photoactive. The interconversion reactions that apply to such membranes are described by eqs 5 and 6:

$$B_s \underset{k_{-3}+k_B(I)}{\overset{k_3}{\rightleftharpoons}} B_w$$

and

$$AB_s \underset{k_{-4}+k_{AB}(I)}{\overset{k_4}{\rightleftharpoons}} AB_w$$

In such membranes, illuminating the feed interface will result in an increase in the concentration of the strong forms of the carrier and complex at that interface (see Figure 1b). The strong forms of the carrier and complex will diffuse to the dark side (the sweep interface) and undergo thermal conversion to the weak form, ultimately resulting in a steep concentration gradient of solute at the sweep interface. Under these conditions, it should be possible to obtain high facilitation factors at fairly high photoefficiencies.

For all the simulations described in this section, the light was incident on the feed interface. The values of ϵ_s and ϵ_w were 0.01, corresponding to fast decomplexation kinetics. The value of α was 50, corresponding to high carrier mobility. The values of ϵ_{car_0} and ϵ_{com_0} were 0.01, corresponding to fast interconversion kinetics, unless otherwise noted. Finally, the value of β was set at 10, a value which corresponded to a high molar absorptivity coefficient.

H. Effects of Binding Constants. Simulations were run for several sets of values for K_s^d and K_w^d in order to explore a range of parameters, and the results are shown in Figure 8. For each set of complexation constants, $K_{car_0} = 100$ and $K_{com_0} = 1$. Facilitation factors greater than 20 could be obtained for values of K_s^d greater than 5. In addition, the degree of facilitation could be modulated by light by factors of 5−10 when K_w^d was small (<1) and the value of K_s^d was in the thermally optimal range (1−10). This trend was expected since the membrane started with the poor transport properties of the weak forms of the carrier and complex and, upon illumination, was converted to a much better transport membrane with the properties of the strong forms of the carrier and complex.

Figure 8a shows the facilitation factors as a function of light intensity for each set of parameters. The maximum facilitation factors obtained were slightly less than those obtained for membranes in which the strong forms were photoactive. However, the degrees of photomodulation were similar to or significantly greater than for the strong form photoactive, as shown in Figure 8b. Furthermore, the maxima in each case occurred at significantly lower light intensities, resulting in photoefficiencies over an order of magnitude greater than membranes in which the strong form was photoactive, as shown in Figure 8c.

The large degree of photomodulation possible with these membranes lies in the differences between K_s^d and K_w^d. This is illustrated in Figure 9, for $K_s^d = 5$, $K_w^d = 0.05$, and $K_{car_0} = 100$. If the interconversion equilibrium constant in the dark strongly favored the weak form of the carrier, then the membrane had the transport properties of the weak form, which were generally rather low. As light initiated conversion of weak form to strong form, the transport properties of the membrane rapidly improved. At the optimal light intensity for photofacilitation, the concentration of the strong form was high at the feed interface, but dropped off at the sweep interface as the strong form thermally converted to the weak form. At high light intensities, the majority of the carrier was in the strong form throughout the membrane, and the transport properties of the membrane were determined by the properties of the strong form of the carrier.

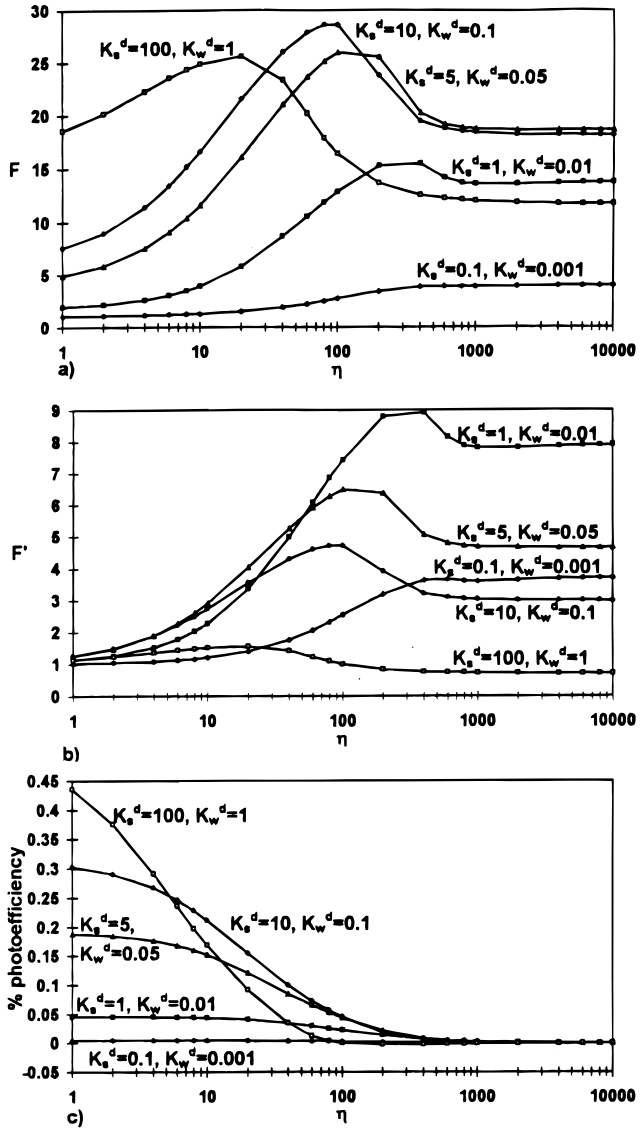

Figure 8. Plots of facilitation, photomodulation, and photoefficiency versus light intensity for different binding constants in liquid membranes in which the weak forms of the carrier and complex were photoactive. For all cases, $\alpha = 50$, $\beta = 10$, $\epsilon_s = \epsilon_w = 0.01$, $\epsilon_{car_0} = \epsilon_{com_0} = 0.01$, $K_{car_0} = 100$, and $K_{com_0} = 1$. Note that the light was incident on the feed interface. (a) Plots of facilitation factor, F, versus light intensity parameter, η, for various sets of K_w^d and K_s^d. (b) Plots of degree of photomodulation, F', versus η for various sets of K_w^d and K_s^d. (c) Plots of % photoefficiency versus η for various sets of K_w^d and K_s^d.

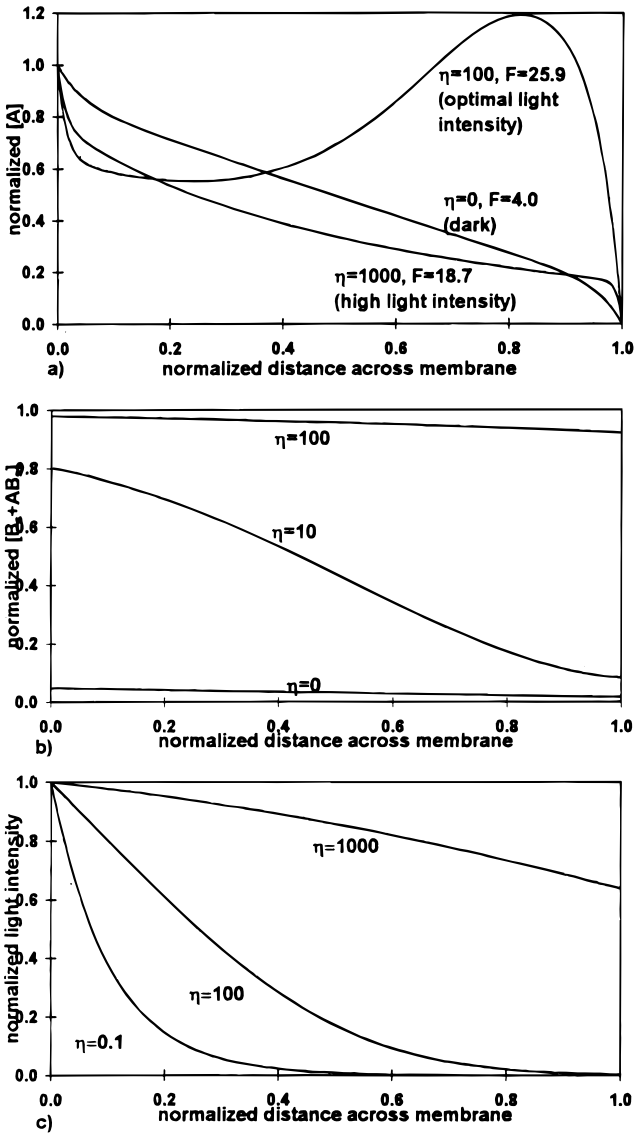

Figure 9. Normalized concentration and light intensity profiles across a membrane in which the weak forms of the carrier and complex were photoactive. For this membrane, $\alpha = 50$, $\beta = 10$, $\epsilon_s = \epsilon_w = 0.01$, $\epsilon_{car_0} = \epsilon_{com_0} = 0.01$, $K_{car_0} = 100$, $K_{com_0} = 1$, $K_s^d = 5$, and $K_w^d = 0.05$. Note that the light was incident at the feed interface. (a) Normalized concentration profiles for the solute, A, across the membrane at various light intensities. (b) Normalized concentration profiles for the sum of the strong forms of the carrier and complex ($B_s + AB_s$) across the membrane at various light intensities. (c) Normalized light intensity profiles across the membrane at various light intensities.

Note that at the light intensity for optimal transport, the normalized concentration profile for the strong forms of the carrier resembled that for the case where the strong form was photoactive (compare Figure 9b and Figure 3b). The total concentration of the strong forms of the carrier and complex was high at the feed and dropped to a much lower concentration at the sweep side, due to thermal conversion to the weak forms. In addition, the light intensity profile at the optimal light intensity was almost the mirror image of the profile at the optimal light intensity when the strong forms of the carrier and complex were photoactive (Figure 3c). The light penetrated all through the membrane, but dropped to nearly zero at the sweep interface.

There is an interesting trend in the magnitude of the light intensity parameter at which the optimal facilitation factor was obtained. In this case, the light intensity necessary to obtain the maximum facilitation factor increased with decreasing values of K_s^d (Figure 8a). Conversely, when the strong forms of the carrier and complex were photoactive, the optimal light intensity increased with increasing values of K_s^d (Figure 2a). The explanation for the opposite trend with weak forms of the carrier and complex being photoactive can be seen in Figure 10, which shows the normalized concentration profiles for the total concentration of strong forms of the carrier and complex for each set of parameters.

Figure 10a shows the normalized concentration profiles for the total amount of the strong forms of the carrier and complex in the dark ($\eta = 0$). Note that the total normalized concentration was significantly higher for the greatest binding constant since the binding equilibrium highly favored the strong form of the complex. At the optimal light intensity for each set of parameters (Figure 10b), the concentrations of the strong forms of the carrier and complex for each set of parameters were very

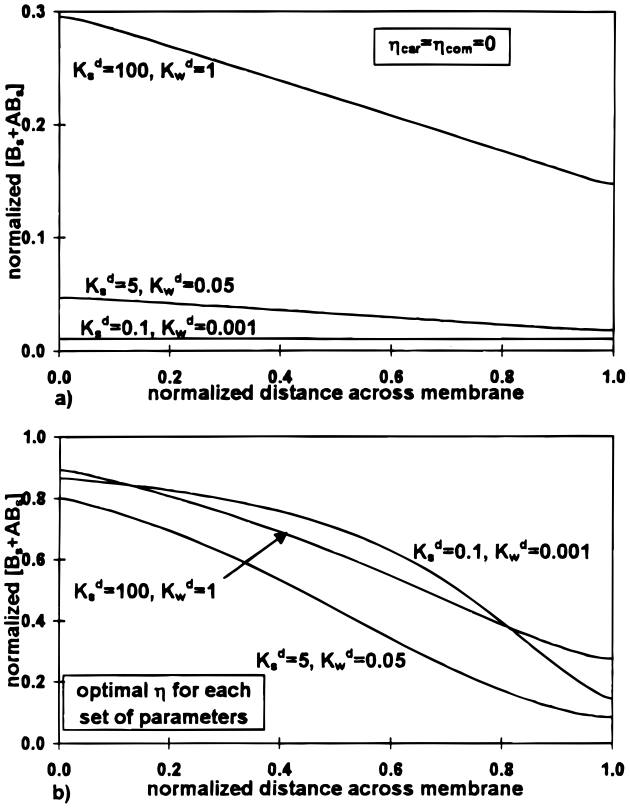

Figure 10. Normalized concentration profiles for the sum of the strong forms of the carrier and complex ($B_s + AB_s$) across the membrane for various sets of binding constants. For all cases, $\alpha = 50$, $\beta = 10$, $\epsilon_s = \epsilon_w = 0.01$, $\epsilon_{car_0} = \epsilon_{com_0} = 0.01$, $K_{car_0} = 100$, and $K_{com_0} = 1$. (a) Normalized concentration profiles in the dark ($\eta = 0$). (b) Normalized concentration profiles at the optimal light intensity parameter for photofacilitation for each set of binding constants.

similar to each other at the feed interface. The same was true at the sweep interface. Since the concentrations of the strong forms of carrier and complex started off higher for the greater binding constants, the optimal concentrations were obtained at lower light intensities. This also resulted in higher photoefficiencies for the higher binding constants.

I. Effects of Weak Binding Constant. The effects of reducing the weak binding constant are shown in Figure 11, where $K_s^d = 5$ and $K_{car_0} = 100$. Varying the value of K_w^d over 3 orders of magnitude had almost no effect on the maximum facilitation factor that could be obtained, unlike membranes in which the strong forms of the carrier and complex were photoactive (Figure 4a). However, reducing K_w^d did significantly increase the degree of photomodulation and slightly increase the photoefficiency. The optimal light intensity for photofacilitation did not change with decreasing K_w^d, whereas the optimal light intensity shifted to higher values with decreasing K_w^d for membranes in which the strong forms of the carrier and complex were photoactive.

J. Effects of Interconversion Equilibrium Constant. Figure 12 illustrates the results of varying the thermal interconversion equilibrium constant between the strong and weak forms of the carrier (K_{car_0}). Below $K_{car_0} = 100$, the maximum facilitation factor obtained and the degree of photomodulation were both rather low, although the photoefficiencies were reasonable. Above $K_{car_0} = 100$, the maximum facilitation factor obtained did not increase much with increasing K_{car_0}. However, the degree of photomodulation increased significantly on going from $K_{car_0} = 100$ to $K_{car_0} = 500$ The photoefficiencies also decreased with the increase in equilibrium constant.

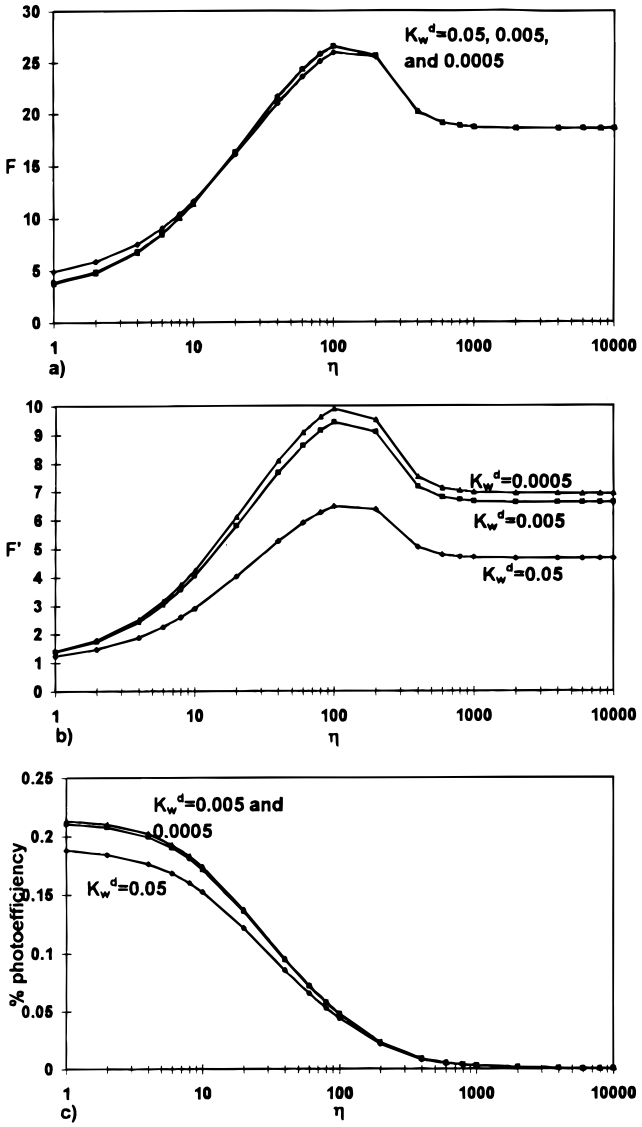

Figure 11. Plots of facilitation, degree of photomodulation, and photoefficiency versus light intensity for various weak binding constants. For all cases, $\alpha = 50$, $\beta = 10$, $\epsilon_s = \epsilon_w = 0.01$, $\epsilon_{car_0} = \epsilon_{com_0} = 0.01$, $K_{car_0} = 100$, and $K_s^d = 5$. (a) Plots of facilitation factor, F, versus light intensity parameter, η, for various K_w^d. (b) Plots of degree of photomodulation, F', versus η for various K_w^d. (c) Plots of % photoefficiency versus η for various K_w^d.

An interesting point is the rather large value of K_{car_0} that was necessary to obtain large degrees of photomodulation. The explanation lies in the effects of the complexation constants on the concentrations of the different forms of the carrier and complex. Since the value of K_s^d was 10 000 times greater than K_w^d, the strong form of the complex was thermodynamically favored over the weak form in the presence of solute. Consequently, in order to have a majority of weak forms of the carrier and complex in the dark, the value of K_{car_0} had to be rather large (>10).

K. Effects of Interconversion Kinetics. The effects of slow interconversion kinetics on photofacilitation and photoefficiency were examined using $K_s^d = 5$, $K_w^d = 0.0005$, and $K_{car_0} = 500$, parameters which provided a high facilitation factor and degree of photomodulation at reasonable photoefficiencies. Figure 13 shows the results of slowing down the rates of interconversion of the strong and weak forms of the carrier and complex by increasing ϵ_{car_0} and ϵ_{com_0}. Reducing the interconversion kinetics

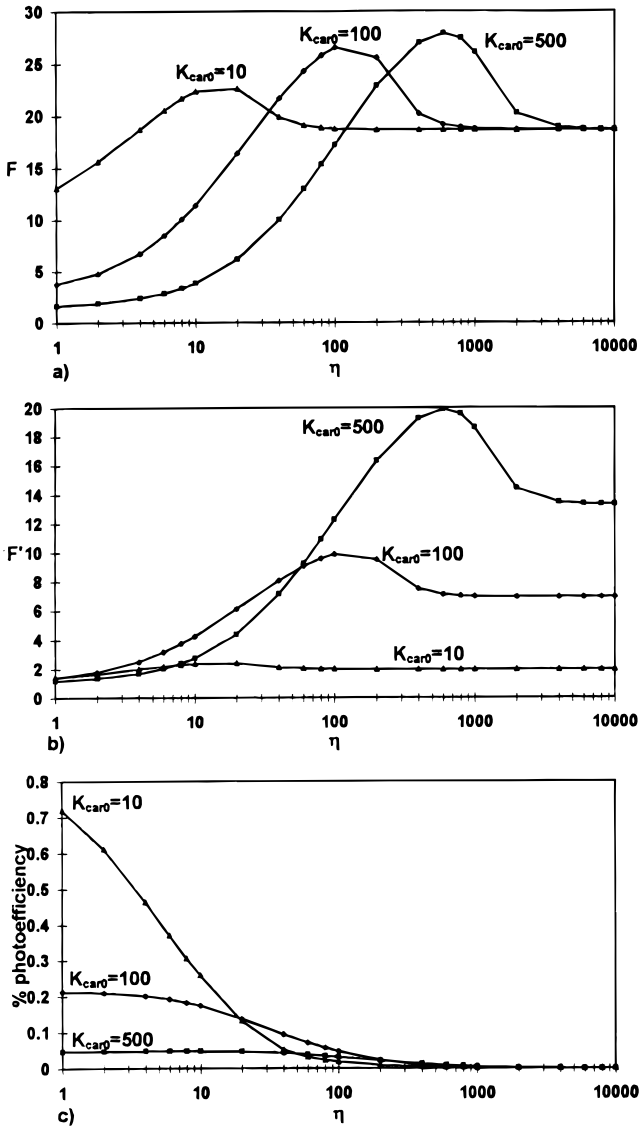

Figure 12. Plots of facilitation, degree of photomodulation, and photoefficiency versus light intensity for various interconversion constants, K_{car_0}. For all cases, $\alpha = 50$, $\beta = 10$, $\epsilon_s = \epsilon_w = 0.01$, $\epsilon_{car_0} = \epsilon_{com_0} = 0.01$, $K_w^d = 0.0005$, and $K_s^d = 5$. (a) Plots of facilitation factor, F, versus light intensity parameter, η, for various K_{car_0}. (b) Plots of degree of photomodulation, F', versus η for various K_{car_0}. (c) Plots of % photoefficiency versus η for various K_{car_0}.

had very little effect on the maximum facilitation factor and degree of photomodulation until ϵ's of 10 and greater were reached (Figure 13a,b). Past values of ϵ_{car_0} and $\epsilon_{com_0} = 10$, the maximum facilitation and degree of photomodulation decreased. However, the photoefficiencies were quite high. Most significantly, much higher photoefficiencies could be obtained than when the strong form of the carrier was photoactive (Figure 13c,d).

L. Summary. Tables 3 and 4 summarize the results of simulations run for photofacilitated liquid membranes in which the weak forms of the carrier and complex were photoactive. Table 3 summarizes results for small K_w^d (<1) and fast interconversion kinetics. Table 4 lists qualitative trends in the maximum facilitation factor, the maximum degree of photomodulation, and the photoefficiency obtained as the listed parameters were varied.

An interesting point to note in Table 4 is that the photoefficiency for photomodulation can be greater than 100% when the weak forms of the carrier and complex are photoactive and

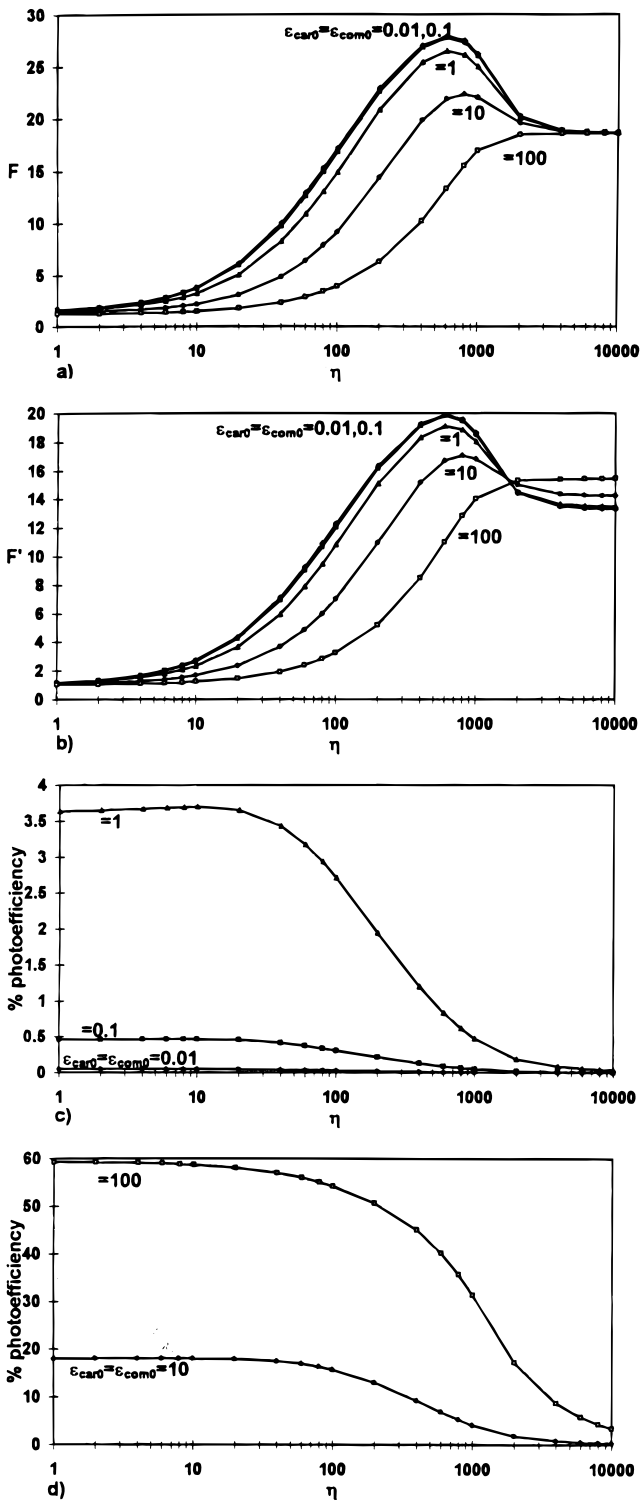

Figure 13. Plots of facilitation, degree of photomodulation, and photoefficiency versus light intensity as the thermal rates of interconversion between strong and weak forms were slowed. For all cases, $\alpha = 50$, $\beta = 10$, $\epsilon_s = \epsilon_w = 0.01$, $K_w^d = 0.0005$, $K_s^d = 5$, $K_{car_0} = 500$, and $K_{com_0} = 0.05$. (a) Plots of facilitation factor, F, versus light intensity parameter, η, for various interconversion rates. (b) Plots of degree of photomodulation, F', versus η for various interconversion rates. (c and d) Plots of % photoefficiency versus η for various interconversion rates.

interconversion kinetics are very slow. In this case, the carrier begins as a very poor facilitator, and solute flux across the membrane is very low. Shining light on the feed interface converts the poor facilitator to a very good facilitator. Since interconversion is very slow, the carrier essentially stays in the

TABLE 3: Weak Forms Photoactive, Light Incident on Feed Interface

range of K_s^d	F_{max}	F'_{max}	% photoefficiency	section
<1	<5	3−4	<0.l	H
1−5	10−25	5−9	0.05−0.2	H, I, J, K
5−10	25−30	4−7	0.2−0.3	H, I, J, K
>10	>25	1−2.5	>0.4	H

TABLE 4: Weak Forms Photoactive, Light Incident on Feed Interface

parameter varied	F_{max}	F'_{max}	% photoefficiency	section
decrease K_w^d	increase	increase	increase	I
decrease K_{car_0}	decrease	decrease	decrease	J
increase ϵ_{car_0} and ϵ_{com_0}	decrease	small decrease	increase (to over 100%)	K

form of the good facilitator, and the membrane is converted to one with good transport properties at a fairly low light intensity. Thus, the solute flux is greatly increased with very few photons wasted.

The optimal characteristics for carriers in which the weak forms are photoactive are somewhat different than when the strong forms are photoactive. To obtain high degrees of photomodulation, the value of K_s^d should be in the thermally optimal range (1−10). Also, K_{car_0} should be rather large (>10). As in the case of membranes in which the strong forms were photoactive, the value of K_w^d should be as small as possible ($K_w^d < 1$).

The differences in the properties of the two types of membranes when the interconversion kinetics were slowed were particularly striking. For both types, reducing the interconversion rates improved the photoefficiency. In the case of membranes in which the strong forms of the carrier and complex were photoactive, the maximum facilitation factor and degree of photomodulation drastically decreased with decreasing interconversion rates. For membranes in which the weak forms of the carrier and complex were photoactive, however, the reduction in the maximum facilitation factor and degree of photomodulation were almost negligible until ϵ_{car_0} and ϵ_{com_0} reached 10. This suggests that the optimal values for ϵ_{car_0} and ϵ_{com_0} would be around 1. In addition, the photoefficiencies were an order of magnitude greater when the weak forms of the carrier and complex were photoactive than when the strong forms were photoactive.

Weak Forms of Carrier and Complex Photoactive, Light Incident on Sweep Interface. Figure 14 depicts typical behavior for membranes in which the weak forms of the carrier and complex were photoactive and the light was incident on the sweep interface. In this case, the behavior of the membrane was very much like a "light switch". In the dark, the transport properties of the membranes were dominated by the binding constants of the weak forms of the carriers and complexes ($K_w^d = 0.01$ in this case), and transport was low. Under illumination, the facilitation factor and the degree of photofacilitation both decreased slightly until a critical light intensity was reached (Figure 14a,b). At this critical light intensity, the facilitation factor and degree of photofacilitation both increased rapidly and then leveled off and remained constant with increasing incident light intensity. At this point, the transport properties were dominated by the binding constant for the strong forms of the carrier and complex ($K_s^d = 1$). The increase in facilitation past the critical light intensity was rather high, a factor of 8 in this case. However, the photoefficiencies were either negative or low (Figure 14c). As in the case of

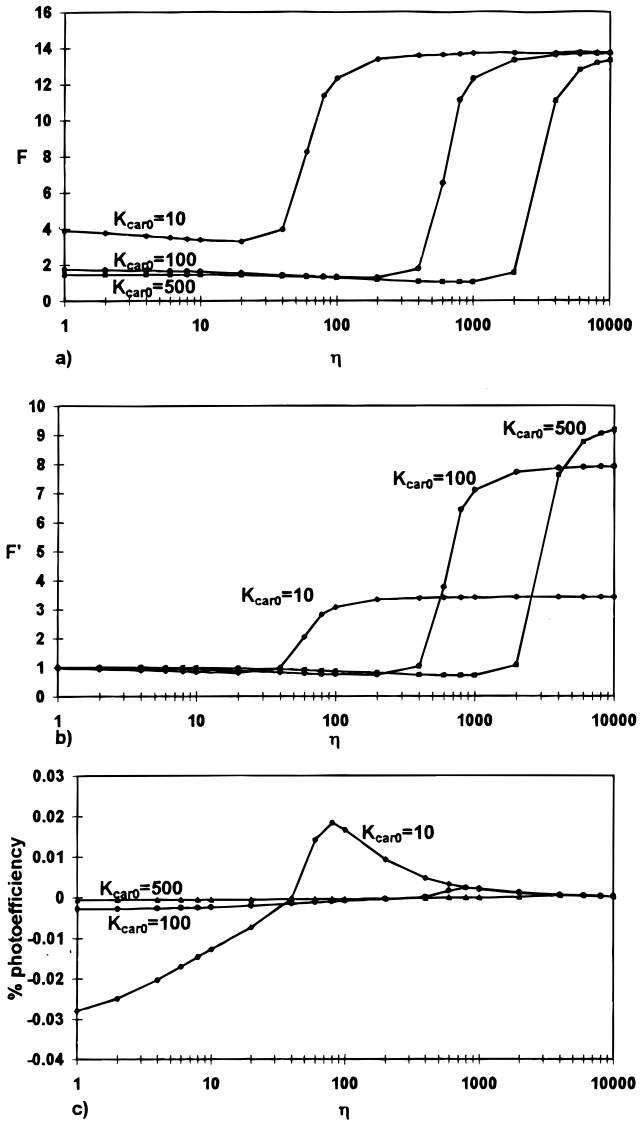

Figure 14. Typical plots of facilitation, degree of photomodulation, and photoefficiency versus light intensity as a function of K_{car_0} for liquid membranes in which the weak forms of the carrier and complex were photoactive and the light was incident on the sweep interface. In this case, $\alpha = 50$, $\beta = 10$, $\epsilon_s = \epsilon_w = 0.01$, $\epsilon_{car_0} = \epsilon_{com_0} = 0.01$, $K_w^d = 0.01$, and $K_s^d = 1$. (a) Plots of facilitation factor, F, versus light intensity parameter, η, for various K_{car_0}. (b) Plots of degree of photomodulation, F', versus η for various K_{car_0}. (c) Plots of % photoefficiency versus η for various K_{car_0}.

membranes in which the weak forms of the carrier and complex were photoactive and light was incident on the feed interface, larger values of K_{car_0} produced much higher degrees of photomodulation than did lower values.

The reasons for the abrupt changes in facilitation are illustrated in Figure 15, which depicts concentration and light intensity profiles for $K_s^d = 1$, $K_w^d = 0.01$, and $K_{car_0} = 100$. As can be seen in Figure 15a, the flux of solute in the dark was due almost entirely to diffusion. At $\eta = 400$, there was a significant concentration of the strong form of the carrier and complex in the membrane, but that mostly served to tie up free solute without enhancing flux. Indeed, the facilitation factor at $\eta = 400$ was almost the same as the facilitation factor in the dark. A slight increase in light intensity to $\eta = 600$ resulted in a significant increase in the facilitation factor. The reason for that abrupt increase is clear in Figure 15b, which depicts normalized concentration profiles for the total amount of strong

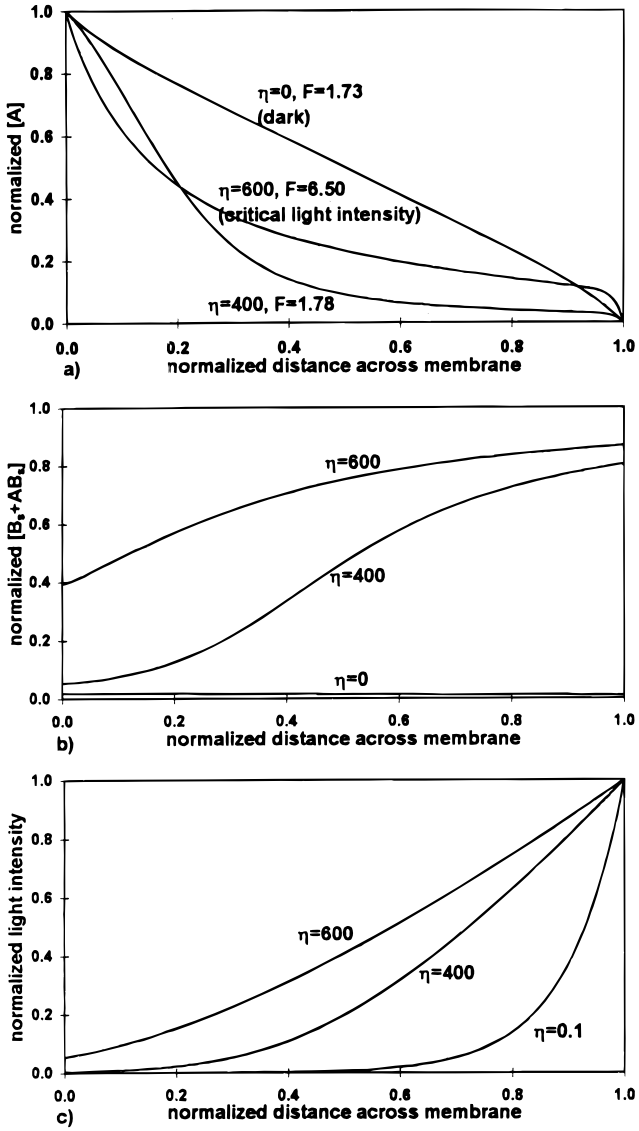

Figure 15. Normalized concentration and light intensity profiles across a membrane in which the weak forms of the carrier and complex were photoactive and light was incident on the sweep interface. For this membrane, $\alpha = 50$, $\beta = 10$, $\epsilon_s = \epsilon_w = 0.01$, $\epsilon_{car_0} = \epsilon_{com_0} = 0.01$, $K_{car_0} = 100$, $K_{com_0} = 1$, $K_s^d = 1$, and $K_w^d = 0.01$. (a) Normalized concentration profiles for the solute, A, across the membrane at various light intensities. (b) Normalized concentration profiles for the sum of the strong forms of the carrier and complex ($B_s + AB_s$) across the membrane at various light intensities. (c) Normalized light intensity profiles across the membrane at various light intensities.

forms of carrier and complex in the membrane. The concentration of strong forms increased by almost an order of magnitude at the feed interface when the light intensity was increased from $\eta = 400$ to $\eta = 600$.

The light intensity profiles, shown in Figure 15c, also reflect the trends in concentrations of the various species. At $\eta = 400$, the light penetrated throughout the membrane, but the intensity dropped to zero at the feed interface. This resulted in conversion of the weak forms of the carrier and complex to the strong forms at the sweep interface but not at the feed interface. When the light intensity was increased to $\eta = 600$, there was significant light intensity at the feed interface, resulting in extensive conversion of the weak to the strong forms of the carrier and complex.

The properties of these membranes can be more easily predicted than for other membranes, since the membrane goes from "off" to "on" with no "bump" in the facilitation factor or photomodulation trends. The strong forms of the carrier and complex should have a binding constant in the thermally optimal range (1−10). The value of the binding constant for the weak forms of the carrier and complex should be as small as possible. The value of K_{car_0} should be as large as possible to ensure that essentially all the carrier and complex are in the weak form in the dark.

Conclusions

Several conclusions can be drawn about optimal parameters for photomodulation in liquid membranes where the strong form of the carrier is photoactive. First, in order to obtain high facilitation factors and high degrees of photomodulation, the value of K_s^d should be greater than the optimal range for thermal facilitated transport (>10), and the value of K_w^d should be less than the optimal range (<1). The greater the separation between the two values, the greater the facilitation factor obtained and the greater the degree of photomodulation.

Variations in the thermal equilibrium constant between the strong and weak forms of the carrier, K_{car_0}, also influenced the degree of photomodulation and photoefficiency. A $K_{car_0} = 1$ provided a reasonably high degree of photomodulation and reasonably high photoefficiencies. Finally, slow interconversion kinetics resulted in about a factor of 10 greater photoefficiencies than fast kinetics, until the interconversion was so slow that the membrane bleached upon illumination and never recovered. However, slow interconversion kinetics resulted in lower facilitation factors and smaller degrees of photomodulation than did fast kinetics.

Something that is important to note is the rapid decrease in the facilitation factor and the degree of photomodulation when the light intensity was increased past the optimal value. In an experimental study, it would be rather easy to start at too high a light intensity, resulting in a photobleached membrane with poor transport properties. When designing an experiment, if interconversion rates are not well-known, it would be important to start at a fairly low light intensity and gradually increase it to find the optimal value.

Some overall conclusions can be drawn about the limits of photofacilitated liquid membranes in which the strong forms of the carrier and complex are photoactive. Fairly high facilitation factors and reasonably large degrees of photomodulation can be obtained by the careful choice of carriers with large differences between the complexation constants for the strong and weak forms of the carrier. The highest facilitation factor obtained in this study was 35; it should be possible to obtain larger facilitation factors, perhaps up to a factor of 2 greater. However, the transport photoefficiencies for such systems will be low, on the order of 0.1% or less. By using carriers with slow interconversion kinetics, it should be possible to obtain photoefficiencies on the order of 5%. However, such systems will not show particularly high facilitation factors or degrees of photomodulation. It appears that in photofacilitated liquid membranes in which the strong forms of the carrier and complex are photoactive, there will generally be a trade-off between photoefficiency and facilitation.

There are several interesting trends in the properties of liquid membranes in which the weak forms of the carrier and complex are photoactive and light is incident on the feed interface. As in the case of membranes in which the strong forms of the carrier and complex were photoactive, the highest facilitation factors were obtained when K_s^d was 5 or greater. However, for values of $K_s^d \geq 1$, the degree of photomodulation generally increased

as the binding constant for the strong forms of the carrier and complex decreased, although values of K_s^d less than 1 fell outside this trend. At low light intensities, photoefficiencies increased with increasing values of K_s^d. Photoefficiencies were generally an order of magnitude greater than for membranes containing photoactive, strong forms of the carrier and complex. In general, very high values of K_{car_0} ($K_{car_0} > 10$) were necessary to obtain high fluxes.

As in the case of membranes with photoactive strong forms of the carrier and complex, decreasing the rate of interconversion increased the photoefficiencies but decreased the maximum facilitation factor obtained. However, decreasing the interconversion rate for membranes with photoactive weak forms of the carrier and complex did not significantly decrease the maximum degree of photomodulation obtained. In addition, at the slowest interconversion rates, photoefficiencies of well over 10% were obtained.

Liquid membranes in which the weak forms of the carrier and complex were photoactive and the light was incident on the sweep interface showed abrupt changes in properties with light intensity. In the dark and at low light intensities, the transport properties of the membranes were dominated by the weak form of the carrier and complex. Past a critical light intensity, the membrane bleached and the transport properties were dominated by the strong forms of the carrier and complex. The conversion was very abrupt and sensitive to light intensity.

It is useful at this point to consider how these parameters, particularly the kinetic parameters, apply to real membrane systems. As was noted very early on, increasing ϵ_s and ϵ_w above values of 0.01 resulted in poor transport properties. Assuming a membrane thickness of $L = 100\ \mu$m and a diffusion coefficient for the complex of $D_{AB} = 1 \times 10^{-6}$ cm^2/s, decomplexation rate constants of 1 s^{-1} for the strong and weak forms of the complex can be calculated from eq 10. Decomplexation rate constants greater than 1 s^{-1} would result in improved transport properties.

The kinetic parameters for interconversion are a different matter. As was noted earlier, the optimal values for ϵ_{car_0} and ϵ_{com_0} were 1 when the weak forms of the carrier and complex were photoactive. Again assuming a membrane thickness of 100 μm and a diffusion coefficient for the complex of 1×10^{-6} cm^2/s, thermal rate constants for the weak form going to the strong form should be on the order of 0.01 s^{-1}. As can be seen in Figure 13, larger rate constants (meaning smaller values of ϵ_{car_0} and ϵ_{com_0}) will not greatly improve the transport properties, but will result in greatly decreased photoefficiencies.

These rate constants are rather low and would apply more to carriers in which photoisomerization occurs, resulting in thermally stable isomers, rather than to carriers that form a photoexcited state. Relaxation processes from photoexcited states have rate constants on the order of 10^3-10^9 s^{-1}, which would result in values of ϵ_{car_0} and ϵ_{com_0} on the order of $10^{-5}-10^{-11}$. Such systems could exhibit high photofacilitation and high degrees of photomodulation, but the photoefficiencies would be vanishingly small.

The optimal rate constants for interconversion can also be used to determine what levels of light intensity would be necessary to obtain good facilitation factors and high degrees of photomodulation. A reasonable set of parameters would be those that were optimal for membranes in which the weak forms of the carrier and complex photoconverted to the strong forms (Figure 13). Those parameters were $K_s^d = 5$, $K_w^d = 0.0005$, $K_{car_0} = 500$, $K_{com_0} = 0.05$, and ϵ_{car_0} and $\epsilon_{com_0} = 1$. For these conditions, the optimal light intensity parameter was $\eta = 600$. A molar absorptivity coefficient of $\tilde{E} = 10^5$ M^{-1} cm^{-1} can be calculated from $\beta = 10$, assuming that the total carrier concentration $C_T = 0.01$ M and the membrane thickness $L = 100\ \mu$m. Using the definition of η_{car} (eq 7) and the previously determined optimal value of $k_{-3} = 0.01$ s^{-1}, an incident photon intensity of $I_0 = 3.6 \times 10^{16}$ photons/(cm^2 s) is determined from the optimal value of η. If a wavelength of 600 nm for initiation of photoconversion is assumed, the power required is 12 mW/cm^2, which is accessible at solar light intensities.

An interesting experimental case to analyze is the spiropyran system studied by Shimidzu and Yoshikawa.[10] In this system, the weak forms of the carrier and complex can be converted to the strong forms with ultraviolet light, while the strong forms can be converted to the weak forms with visible light. All forms of the carrier and complex were thermally stable. The investigators actually ran membrane transport experiments by converting the strong forms to the weak forms and observed photomodulation of the transport of solute of a factor of 2.

Shimidzu and Yoshikawa determined that the thermal rate constant for the photoisomerization of the strong form of the carrier to the weak form was $k_{-3} = 4.4 \times 10^{-3}$ s^{-1}. The authors did not report a membrane thickness or a diffusion coefficient for the complex, but the value of k_{-3} they report would provide an ϵ_{car_0} of about 2, assuming $L = 100\ \mu$m and $D_{AB} = 10^{-6}$ cm^2/s. This value is certainly in the right range to provide good facilitation and photomodulation with reasonable photoefficiencies. However, the equilibrium constant between the strong form and the weak form of the carrier was only 0.075, which was rather low. In addition, the difference between the strong and weak binding constants was only a factor of 2, at best. Under such conditions, little photofacilitation would be expected, and only a low degree of photomodulation was actually observed.

Appendix

Various assumptions and parameters for the model not fully described above are included here. It is assumed that the photoactive forms of the carrier and complex absorb light of the same narrow wavelength range in undergoing conversion to the photoinactive forms and that the photoinactive forms do not absorb light in the same range. While this assumption is made to reduce the number of variables and simplify the calculations, it is not too far from physical reality for many potential carriers. Absorption factors for the photoinactive forms could be easily included in the model for specific cases. Finally, the possibility of stimulated emission from the photoinactive forms of the carrier and complex is assumed to be negligible.

If it is assumed that the diffusion coefficients for all forms of the carrier and the complex are the same and do not vary across the membrane, then

$$C_T = [B_w] + [B_s] + [AB_w] + [AB_s] \tag{24}$$

where C_T is the total concentration of carrier (both free and complexed) in the membrane. This insures that the total concentration of carrier is constant across the membrane.

The following boundary conditions apply:

at $x = 0$, $[A] = [A]_0$,

$$\frac{d[B_w]}{dx} = \frac{d[B_s]}{dx} = \frac{d[AB_w]}{dx} = \frac{d[AB_s]}{dx} = 0 \tag{25}$$

at $x = L$, $[A] = [A_L] = 0$,

$$\frac{d[B_w]}{dx} = \frac{d[B_s]}{dx} = \frac{d[AB_w]}{dx} = \frac{d[AB_s]}{dx} = 0 \tag{26}$$

Under these conditions, all forms of the carrier are nonvolatile and confined within the membrane. The conditions on A indicate that there is a constant source of A at $x = 0$ (the feed side) and that A is removed from the membrane at $x = L$ (the sweep side) such that the concentration at the sweep interface remains constant. There is also one boundary condition on the light. If the light is incident on the sweep interface of the membrane, then

$$\text{at } x = L, \quad I = I_0 \tag{27}$$

Conversely, if the light is incident on the feed interface of the membrane, then

$$\text{at } x = 0, \quad I = I_0 \tag{28}$$

In addition, at steady state, the total flux of A is constant across the membrane.

$$J_A = -D_A \frac{d[A]}{dx} - D_{AB} \frac{d[AB_w]}{dx} - D_{AB} \frac{d[AB_s]}{dx} \tag{29}$$

The equations and parameters are converted to dimensionless form to clarify and generalize photofacilitation effects. The dimensionless parameters and variables are

$$\bar{A} = \frac{[A]}{[A]_0}, \quad \overline{B_w} = \frac{[B_w]}{C_T}, \quad \overline{B_s} = \frac{[B_s]}{C_T},$$
$$\overline{AB_w} = \frac{[AB_w]}{C_T}, \quad \overline{AB_s} = \frac{[AB_s]}{C_T}, \quad \chi = \frac{x}{L} \tag{30}$$

$$\epsilon_w = \frac{D_{AB}}{L^2 k_{-1}}, \quad \epsilon_s = \frac{D_{AB}}{L^2 k_{-2}},$$
$$\epsilon_{car_0} = \frac{D_{AB}}{L^2 k_{-3}}, \quad \epsilon_{com_0} = \frac{D_{AB}}{L^2 k_{-4}} \tag{31}$$

$$K_w^d = \frac{k_1}{k_{-1}}[A]_0, \quad K_s^d = \frac{k_2}{k_{-2}}[A]_0,$$
$$K_{car_0} = \frac{k_3}{k_{-3}}, \quad K_{com_0} = \frac{k_4}{k_{-4}} \tag{32}$$

$$\alpha = \frac{D_{AB} C_T}{D_A [A]_0} \tag{33}$$

The dimensionless parameters and variables involving light are

$$\bar{I} = \frac{I}{I_0} \tag{34}$$

$$\eta_{car} = \frac{\Phi_B E_B I_0}{k_{-3}}, \quad \eta_{com} = \frac{\Phi_{AB} E_{AB} I_0}{k_{-4}} \tag{35}$$

$$\epsilon_{car}(I) = \frac{D_{AB}}{L^2(k_{-3} + k_B(I))} = \frac{\epsilon_{car_0}}{1 + \eta_{car}\bar{I}},$$
$$\epsilon_{com}(I) = \frac{\epsilon_{com_0}}{1 + \eta_{com}\bar{I}} \tag{36}$$

$$K_{car}(I) = \frac{k_3}{k_{-3} + k_B(I)} = \frac{K_{car_0}}{1 + \eta_{com}\bar{I}},$$
$$K_{com}(I) = \frac{K_{com_0}}{1 + \eta_{com}\bar{I}} \tag{37}$$

$$\beta_{car} = \tilde{E}_B C_T L, \quad \beta_{com} = \tilde{E}_{AB} C_T L \tag{38}$$

Here, Φ represents the quantum yield for conversion of the photoactive form of carrier (or complex) to the photoinactive form of carrier (or complex) in units of mol of photoactive form converted/mol of photons absorbed. E represents molar absorptivity in units of cm^2/mol. $\tilde{E}$ represents molar absorptivity in units of L/(mol cm). I_0 is the incident light intensity in units of mol of photons/(cm^2 s).

A dimensionless flux can also be defined as

$$N_{\bar{A}} = -\frac{d\bar{A}}{d\chi} - \alpha \frac{d\overline{AB_w}}{d\chi} - \alpha \frac{d\overline{AB_s}}{d\chi} \tag{39}$$

It is important to note that not all of the parameters are independent of each other. Defining three of the four equilibrium constants is sufficient to determine the fourth. For the case in which the strong forms of the carrier and complex are photoactive,

$$K_{com_0} = \frac{K_{car_0} K_s^d}{K_w^d} \tag{40}$$

For the case in which the weak forms of the carrier and complex are photoactive,

$$K_{com_0} = \frac{K_{car_0} K_w^d}{K_s^d} \tag{41}$$

In addition, each η term is related to the other through ϵ_{car_0}, ϵ_{com_0}, β_{car}, and β_{com}. Generally, when solving the equations, η_{car}, ϵ_{car_0}, ϵ_{com_0}, β_{car}, and β_{com} were defined and η_{com} was calculated as

$$\eta_{com} = \frac{\Phi_{AB} \eta_{car} \epsilon_{com_0} \beta_{com}}{\Phi_B \epsilon_{car_0} \beta_{car}} \tag{42}$$

Throughout the calculations, Φ_B and Φ_{AB} were set equal to 1. Many potential carriers have high quantum yields for conversion, so the approximation of setting Φ_B and Φ_{AB} equal to 1 is not unreasonable. However, if the quantum yields for conversion are much less than 1, then the incident light intensity necessary to achieve a certain effect at a given η_{car} or η_{com} will be proportionally greater.

Since coupled second-order differential equations such as the mass transport equations which apply to this system generally do not have analytical solutions, numerical methods are necessary to solve for concentration and flux profiles. The FORTRAN program BVPFD (from the IMSL library) was used to obtain solutions. Details on how this program was used to solve the equations are given in a previous paper.[16] This program does allow the use of a logarithmic x grid, providing closely

spaced x points at the edges and wider spacing in the center. A description of the grid resolution is given in a previous paper.[16] The minimum number of grid points needed in order to always obtain convergence was 201 for the sets of parameters used in this study.

List of Parameters and Variables

parameter	definition	description	eqs
k_1		rate constant for complexation for weak form of carrier	
k_{-1}		rate constant for decomplexation for weak form of complex	
k_2		rate constant for complexation for strong form of carrier	
k_{-2}		rate constant for decomplexation for strong form of complex	
k_3		rate constant for thermal conversion of photoinactive form of carrier to photoactive form of carrier	
k_{-3}		rate constant for thermal conversion of photoactive form of carrier to photoinactive form of carrier	
k_4		rate constant for thermal conversion of photoinactive form of complex to photoactive form of complex	
k_{-4}		rate constant for thermal conversion of photoactive form of complex to photoinactive form of complex	
$k_B(I)$	$\Phi_B E_B I_0$	light intensity dependent rate constant for conversion of photoactive form of carrier to photoinactive form of carrier	(7)
$k_{AB}(I)$	$\Phi_{AB} E_{AB} I_0$	light intensity dependent rate constant for conversion of photoactive form of complex to photoinactive form of complex	(8)
$[A]_0$		concentration of solute at feed interface	
C_T		total concentration of carrier in membrane	(24)
L		membrane thickness	
x		distance across membrane	
D_{AB}		diffusion coefficient for all forms of carriers and complexes in the membrane	
D_A		diffusion coefficient for solute in the membrane	
Φ_B		quantum yield for conversion of photoactive form of carrier to photoinactive form	
Φ_{AB}		quantum yield for conversion of photoactive form of complex to photoinactive form	
E_B		molar absorptivity coefficient for photoactive form of carrier in cm^2/mol	
E_{AB}		molar absorptivity coefficient for photoactive form of complex in cm^2/mol	
$\tilde{E}_B$		molar absorptivity coefficient for photoactive form of carrier in $M^{-1}\ cm^{-1}$	
$\tilde{E}_{AB}$		molar absorptivity coefficient for photoactive form of complex in $M^{-1}\ cm^{-1}$	
$\bar{A}$	$[A]/[A]_0$	normalized concentration of free solute in membrane	(10)
$\bar{B}_w$	$[B_w]/C_T$	normalized concentration of weak form of carrier in membrane	(11) (30)
$\bar{B}_s$	$[B_s]/C_T$	normalized concentration of strong form of carrier in membrane	(30)
$\overline{AB}_w$	$[AB_w]/C_T$	normalized concentration of weak form of complex in membrane	(11) (30)
$\overline{AB}_s$	$[AB_s]/C_T$	normalized concentration of strong form of complex in membrane	(30)
$\bar{\chi}$	x/L	normalized distance across membrane	(30)
$\bar{I}$	I/I_0	normalized light intensity	(34)
α	$D_{AB}C_T/(D_A A_0)$	mobility parameter	(14) (33)
η_{car}	$\Phi_B E_B I_0/k_{-3}$	light intensity parameter for carrier	(9) (35)
η_{com}	$\Phi_{AB} E_{AB} I_0/k_{-4}$	light intensity parameter for complex	(9) (35) (42)
K_w	k_1/k_{-1}	binding constant for weak form of carrier	(1)
K_s	k_2/k_{-2}	binding constant for strong form of carrier	(2)
K_w^d	$(k_1/k_{-1})[A]_0$	dimensionless binding constant for weak form of carrier	(13) (32)
K_s^d	$(k_2/k_{-2})[A]_0$	dimensionless binding constant for strong form of carrier	(13) (32)
K_{car_0}	k_3/k_{-3}	thermal interconversion constant between strong and weak forms of carrier	(17) (32)
K_{com_0}	k_4/k_{-4}	thermal interconversion constant between strong and weak forms of complex	(17) (32) (40) (41)
$K_{car}(I)$	$K_{car_0}/(1+\eta_{car}\bar{I})$	light intensity dependent interconversion constant between strong and weak forms of carrier	(3) (5) (18) (37)
$K_{com}(I)$	$K_{com_0}/(1+\eta_{com}\bar{I})$	light intensity dependent interconversion constant between strong and weak forms of complex	(4) (6) (18) (37)
ϵ_w	$D_{AB}/(L^2 k_{-1})$	kinetic parameter for weak forms of carrier and complex	(12) (31)
ϵ_s	$D_{AB}/(L^2 k_{-2})$	kinetic parameter for strong forms of carrier and complex	(12) (31)
ϵ_{car_0}	$D_{AB}/(L^2 k_{-3})$	thermal kinetic parameter for interconversion between strong and weak forms of carrier	(15) (31)
ϵ_{com_0}	$D_{AB}/(L^2 k_{-4})$	thermal kinetic parameter for interconversion between strong and weak forms of complex	(15) (31)
$\epsilon_{car}(I)$	$\epsilon_{car_0}/(1+\eta_{car}\bar{I})$	light intensity dependent kinetic parameter for interconversion between strong and weak forms of carrier	(16) (36
$\epsilon_{com}(I)$	$\epsilon_{com_0}/(1+\eta_{com}\bar{I})$	light intensity dependent kinetic parameter for interconversion between strong and weak forms of complex	(16) (36)
β_{car}	$C_T\tilde{E}_B L$	normalized molar absorptivity coefficient for photoactive form of carrier	(19) (38)
β_{com}	$C_T\tilde{E}_{AB} L$	normalized molar absorptivity coefficient for photoactive form of complex	(19) (38)
		Parameters for Characterizing Transport	
$N_{\bar{A}}$	$-(d\bar{A}/d\chi) - \alpha(d\overline{AB}_w/d\chi) - \alpha(d\overline{AB}_s/d\chi)$	total dimensionless flux of solute	
F	$N_{\bar{A},carrier}/N_{\bar{A},no\ carrier}$	facilitation factor	(20)
F'	$N_{\bar{A},light}/N_{\bar{A},dark}$	degree of photomodulation	(21)
Ψ	$(\beta_{com}\epsilon_{com_0}/\alpha\eta_{com}) \times (N_{\bar{A},light} - N_{\bar{A},dark}) \times 100$	% photoefficiency	(22) (23)

Acknowledgment. This research was supported by the Dept. of Energy (BES) Solar Photochemistry Program, Grant DE-FGO3-94ER14434.

References and Notes

(1) Halwachs, W.; Schügerl, K. *Int. Chem. Eng.* **1980**, *20*, 519.
(2) Way, J. D.; et al. *J. Membr. Sci.* **1982**, *12*, 239.
(3) Schultz, J. S. *Science* **1977**, *197*, 1177.
(4) Haberfield, P. *J. Am. Chem. Soc.* **1987**, *109*, 6178.
(5) Ino, M.; et al. *J. Membr. Sci.* **1994**, *89*, 101.
(6) Irie, M.; Kato, M. *J. Am. Chem. Soc.* **1985**, *107*, 1024.
(7) Jain, R.; Schultz, J. S. *J. Membr. Sci.* **1986**, *26*, 313.
(8) Sasaki, H.; Ueno, A.; Osa, T. *Bull. Chem. Soc. Jpn.* **1988**, *61*, 2321.
(9) Sasaki, H.; Ueno, A.; Osa, T. *Chem. Lett.* **1986**, 1785.
(10) Shimidzu, T.; Yoshikawa, M. *J. Membr. Sci.* **1983**, *13*, 1.
(11) Shinkai, S.; et al. *J. Chem. Soc., Perkin Trans 1* **1981**, 3279.
(12) Shinkai, S.; et al. *J. Chem. Soc., Perkin Trans. 1* **1982**, 2735.
(13) Shinkai, S.; et al. *J. Am. Chem. Soc.* **1982**, *104*, 1967.
(14) Shinkai, S.; Miyazaki, K.; Manabe, O. *J. Chem. Soc., Perkin Trans. 1* **1987**, 449.
(15) Jain, R.; Schultz, J. S. *J. Membr. Sci.* **1983**, *15*, 63.
(16) Longin, T. L.; Koval, C. A.; Noble, R. D. *J. Phys. Chem. B* **1997**, *101*, 7172.
(17) Ruckenstein, E.; Sasidhar, V. *J. Membr. Sci.* **1982**, *12*, 27.
(18) Smith, D. R.; Lander, R. J.; Quinn, J. A. In *Recent Developments in Separation Science:* Li, N. D., Eds.; CRC Press: Cleveland, OH, 1977; p 2.
(19) Kemena, L. L.; Noble, R. D.; Kemp, N. J. *J. Membr. Sci.* **1983**, *15*, 259.